Article:
Provis, J.L., Palomo, A. and Shi, C. (2015) Advances in understanding alkali-activated materials. Cement and Concrete Research, 78 (Part A). pp. 110-125. ISSN 0008-8846

https://doi.org/10.1016/j.cemconres.2015.04.013

Preprint of: JL Provis, A Palomo, C Shi, Advances in understanding alkali-activated materials, *Cement and Concrete Research*, 78A (2015): 110-125. Final published version is available at http://dx.doi.org/10.1016/j.cemconres.2015.04.013

Advances in understanding alkali-activated materials

John L. Provis[1], Angel Palomo[2], Caijun Shi[3]

[1] Department of Materials Science & Engineering, University of Sheffield, Sheffield S1 3JD, United Kingdom. Email j.provis@sheffield.ac.uk

[2] Department of Cements and Materials Recycling , Instituto de Ciencias de la Construcción Eduardo Torroja (IETcc-CSIC), Madrid, Spain. Email palomo@ietcc.csic.es

[3]* College of Civil Engineering, Hunan University, Changsha, China. Email cshi@hnu.edu.cn

Abstract

Alkali activation is a highly active and rapidly developing field of activity in the global research and development community. Commercial-scale deployment of alkali-activated cements and concretes is now proceeding rapidly in multiple nations. This paper reviews the key developments in alkali-activated materials since 2011, with a particular focus on advances in characterisation techniques and structural understanding, binder precursors and activation approaches, durability testing and design, processing, and sustainability. The scientific and engineering developments described in this paper have underpinned the on-going scale-up activities. We also identify important needs for future research and development to support the optimal and appropriate utilisation of alkali activated materials as a component of a sustainable future construction materials industry.

Keywords: Alkali-activated material (D); binder precursor; structural characterization (D); durability (C); sustainability

*Corresponding author:Caijun Shi, cshi@hnu.edu.cn; +86 731-88823937

Preprint of: JL Provis, A Palomo, C Shi, Advances in understanding alkali-activated materials, *Cement and Concrete Research*, 78A (2015): 110-125. Final published version is available at http://dx.doi.org/10.1016/j.cemconres.2015.04.013

1. Introduction

The keynote paper dedicated to the 13th International Congress on the Chemistry of Cement held in Madrid in 2011 focused on the chemistry of alkali-activated and hybrid binder systems [1]. The aim of this paper is not to provide a detailed overview of all aspects of the history, chemistry and engineering of alkali-activated materials (AAMs), which can be found in references [2-6]. Nor does it aim to summarise in detail the extensive published work in validating the use of different sources of fly ash, blast furnace slag and metakaolin in AAMs, a topic which comprises a very large percentage of the publications in this field. Rather, it is intended to review and highlight the key recent scientific developments in the development, characterisation, durability, processing and environmental assessment of AAMs since the last Congress.

2. Advances in characterisation

The characterisation of cementitious materials is well known to present significant challenges when applying most common materials science techniques. The disordered, chemically complex, multiphase nature of the key strength-giving components of cementitious materials means that the parameters controlling their structure have only recently been understood in detail. This is further complicated by the fact that most precursor materials used in AAMs are also structurally disordered, being either glassy (e.g. fly ash; blast furnace slag) or thermally disrupted layer structures (e.g. metakaolin and other calcined clays). This means that the contribution of unreacted precursors to an observed spectrum or diffractogram, which must be accounted accurately in any truly quantitative analysis, is often difficult to identify and delineate [7, 8]. This remains probably the most significant outstanding problem in the structural analysis of AAMs. The advances in both in situ and ex situ characterisation techniques during the past several years have brought a much deeper understanding of both the nanostructure and the microstructure of AAMs. This section summarises application of these techniques to the study of AAMs.

2.1 Nanostructural characterisation

The nanostructure of AAMs is strongly dependent on the available calcium content of precursors; a high-calcium system such as alkali-activated blast furnace slag is dominated by a calcium aluminosilicate hydrate (C-A-S-H) gel with a tobermorite-like (mostly Q^2, some Q^1 and Q^3) structure [3, 9], while low-calcium systems such as those based on metakaolin or fly ash tend to generate an alkali aluminosilicate (N-A-S-H) gel with a highly crosslinked (mainly Q^4), disordered pseudo-zeolitic structure [3, 10, 11]. These gels can coexist in binders based on blends of high-calcium and low-calcium precursors [12-14], although the stability of the gel coexistence at high alkalinity is still the subject of some discussion[5, 15, 16]; Garcia-Lodeiro et al. [16] found a tendency towards C-A-S-H gel as the final stable product when the pH remained >12in mixtures of synthetic C-S-H and N-A-S-H gels.

The key spectroscopic techniques which are used in analysis of AAMs include Fourier transform infrared (FTIR) and nuclear magnetic resonance (NMR) spectroscopy. The majority of published NMR studies of AAMs investigate ^{27}Al and ^{29}Si nuclei by a magic angle spinning (MAS) approach, which yields information about the coordination states of Al and the connectivity of Si (to non-bridging oxygen sites, or bridges to Si or Al). Such information has been instrumental in building a deeper understanding of the network structures of both C-A-S-H and N-A-S-H gels in AAMs [8, 17-19]. Many attempts have been made to quantify the contributions of component sub-peaks to measured NMR spectra of AAMs using mathematical deconvolution processes. However, it is essential to note that unless the contribution of the remnant unreacted precursor is taken correctly into account – either

through selective isotopic labelling of the binder [20], or through subtraction of a scaled component spectrum for the remnant precursor during the deconvolution process (Figure 1) [8, 18, 21] – the quantification of the spectra will not yield an accurate representation of the binder chemistry.

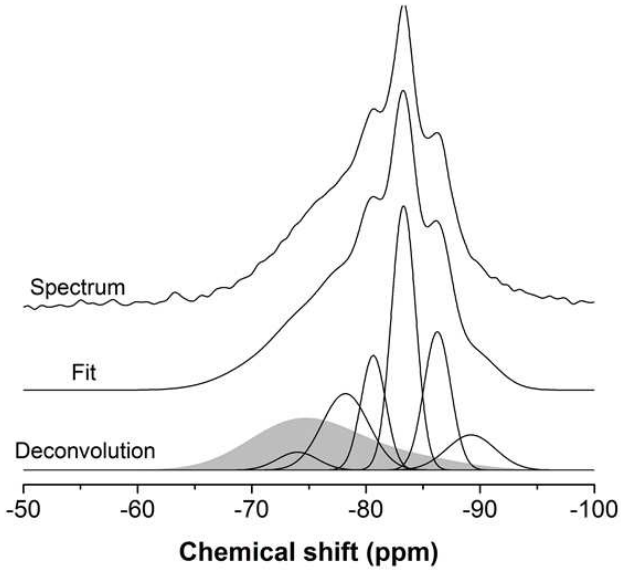

Figure 1.^{29}Si MAS NMR spectrum of a sodium metasilicate-activated blast furnace slag paste cured for 14 days, with deconvolution into component peaks. The fit is the sum of the deconvoluted peaks, and the dark grey band represents the contribution of the remnant anhydrous slag. Adapted from [18].

Two-dimensional NMR approaches such as multiple quantum MAS NMR, probing quadrupolar nuclei including ^{17}O, ^{23}Na and ^{27}Al [20, 22, 23], are starting to bring additional insight into the details of the bonding environments within the N-A-S-H gel in particular, and appear to offer significant scope for future advances in the understanding of AAMs. Less common nuclei such as ^{43}Ca, ^{39}K and ^{25}Mg can also yield useful information if studied at sufficiently high magnetic field [24-26], although interpretation of the spectra is not always straightforward. The significant Fe content of most fly ashes can limit the resolution and spectral quality achievable for those materials, but spectra of excellent quality are in general able to be obtained for materials based on slags and metakaolin.

Infrared spectroscopy is a key technique for the analysis of AAMs, particularly for low-calcium systems where it can probe the connectivity within Si-O-(Si,Al) frameworks via shifts in the peak corresponding to the asymmetric stretch of that bond [27-29]. Recent developments in the application of infrared spectroscopy have involved the use of in situ time-resolved FTIR spectroscopy, where spectra are collected as often as every minute during a reaction process [30, 31], and also infrared microscopy (often conducted using a synchrotron beamline source), which enables collection of spatially-resolved infrared data for polished samples[31]. The combination of time-resolved and spatially resolved infrared spectroscopy has also provided powerful new insight into the influence of the availability of the binder-forming species silica [32] and alumina [33] on gel structures. The theory of an initial Al-rich binder gel (described as "Gel 1") forming at early age, and then evolving to a more Si-rich structure ("Gel 2"), which was developed from ex-situ analysis of the gel evolution [27], has also been refined. As FTIR spectroscopy measures bond vibrations rather than the actual nuclei, the distinction between 'Al-rich' and 'Si-rich' gels is related to connectivity rather than bulk composition: the 'Gel 1' stage involves a high degree of formation of Si-O-Al bonds relative to the bulk Si/Al ratio, because the formation of crosslinks involving Al atoms joining between Si sites is rapid. This leads to a gel which has a relatively high concentration of Si-O-Al bonds. Later, the ongoing gel structural evolution

involves condensation reactions between the Si-OH groups remaining within the immature gel, giving an increase in the effective Si/Al ratio of the gel as measured by FTIR[5]. This explains why the gel formed by the reaction between a solid aluminosilicate precursor (e.g. fly ash) and a silicate activator – which has a very high Si/Al ratio in the solution phase at early age – can appear relatively 'Al-rich' to FTIR spectroscopy at early age, when bulk chemical considerations would indicate that the Si/Al ratio should decrease throughout the reaction process as Al is gradually released from the fly ash particles, and the additional Si supplied by the activator is consumed.

Pair distribution function (PDF) analysis, as reviewed by Meral et al.[34], involves the calculation of interatomic distance correlations for disordered materials from 'total scattering' data. The use of X-ray and neutron PDF analysis in the study of AAMs has continued to provide unparalleled new insight into the formation and structure of the gels which dominate these materials [35].*In situ* PDF analysis (Figure 2) provides direct insight into the molecular-scale structural development of the disordered binder phases on a timescale which can be as short as 3 minutes when using a synchrotron beamline source [36], or 15 minutes for a high-intensity neutron scattering instrument [37]. *Ex situ* analysis of as-synthesised and thermally-treated samples has also provided new understanding of the structure of metakaolin and the products of its alkali-activation [38, 39], and the differences between the C-A-S-H gels formed by hydration of Portland cement and in alkali-activation of blast furnace slag [40].

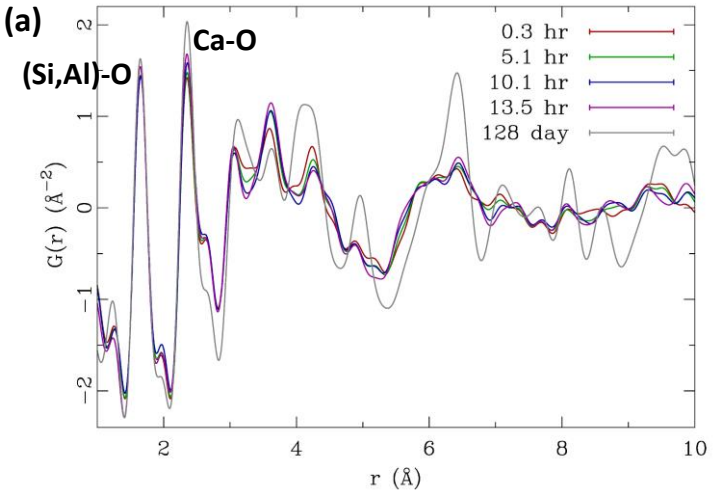

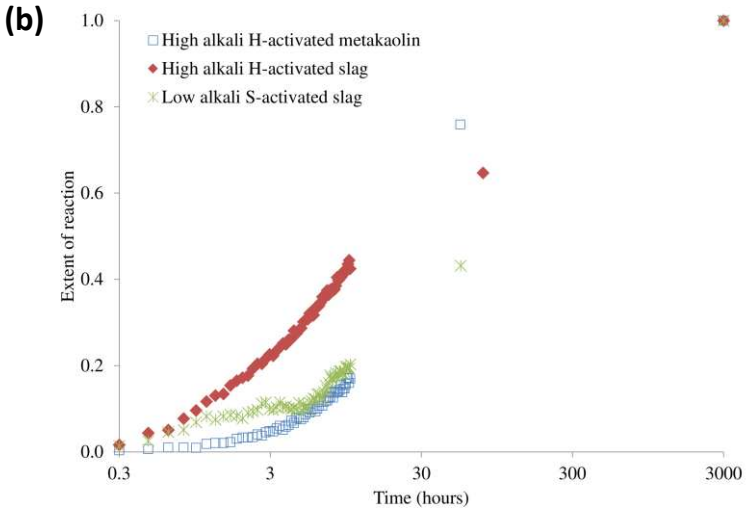

Figure 2. (a) X-ray PDF data for sodium silicate activation of slag, collected *in situ* at times as marked, and with the atomic interactions responsible for the nearest-neighbour peaks identified; (b) quantification of the *in situ* PDF data collected for sodium hydroxide ('H') and sodium silicate ('S') activation of metakaolin and slag, normalised to 100% extent of reaction at128 days (approx. 3000 hours) for all systems. Adapted from [36].

Recent developments in the understanding of the C-A-S-H gel in alkali-activated blast furnace slag binders have been focused on the construction of a realistic structural description of the silicate chain structures in this gel, which can differ significantly from those formed in the C-S-H produced by Portland cement hydration [40-42]. This is mainly attributed to the low Ca/Si ratio and high Al content of the gel produced by alkali activation of blast furnace slag, which opens the possibility of cross-linking between the *dreierketten* chains of the tobermorite-like gel [19, 41], Figure 3.

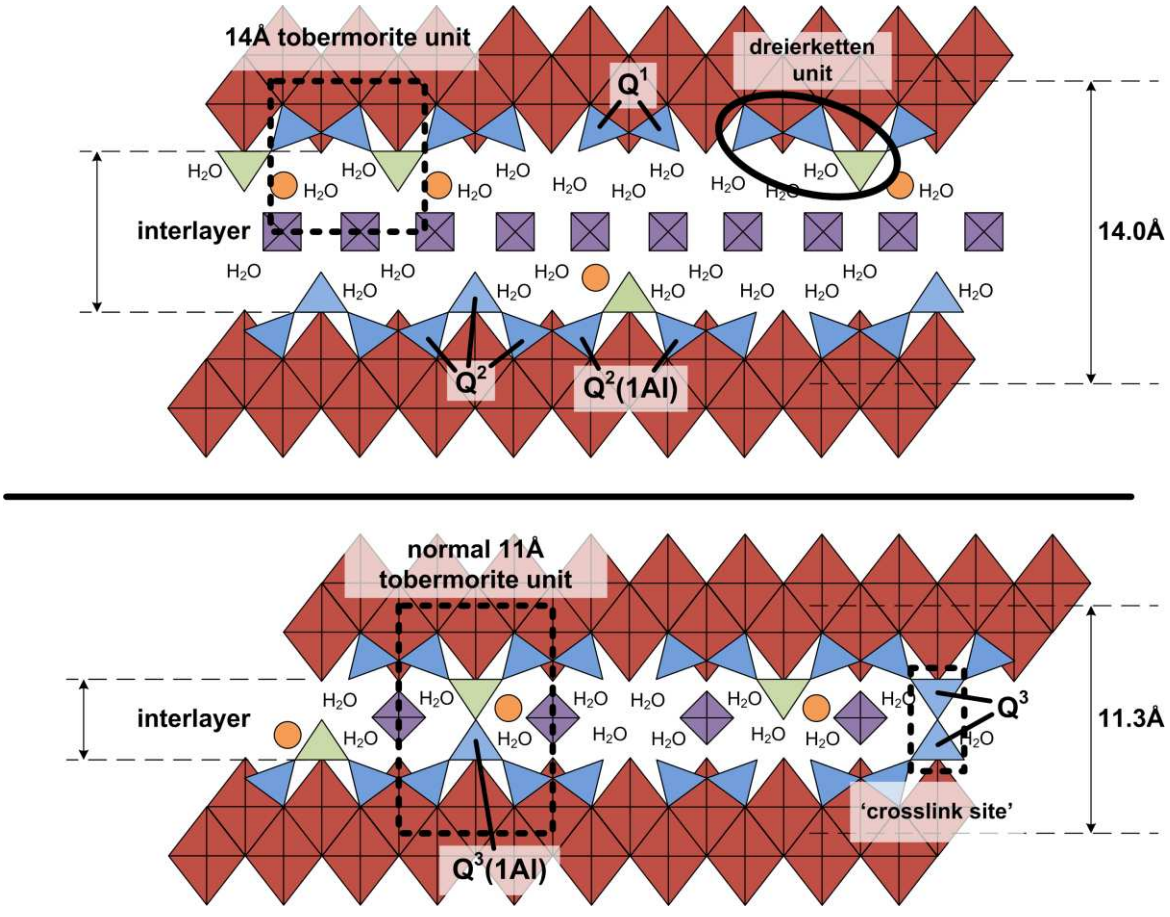

Figure 3.Schematic of structural features, silicate and aluminate site environments, cross-linking, and interlayer sites in tobermorite-like C-N-A-S-H. Adapted from [41].

The question of whether the alkali metal cations in AAMs can become structurally incorporated into C-A-S-H, or are mainly sorbed onto its surface, is yet to be fully resolved. This is partially related to the difficulty in defining what exactly is the 'surface' of such a small (a few nanometres) particle, and partially also due to challenges in distinguishing ion-exchangeable interlayer sites from ion-exchangeable surface sites via currently-available analytical techniques. However, the determination of pore solution chemistry in alkali-activated slag, and its comparison with solubility measurements carried out in more dilute solutions, show that alkali uptake by the gels is a function of gel chemistry rather than being dominated by the available surface area [43]. This shows that the incorporation of the alkalis into the gel structure is significant, and may provide at least a partial explanation for recent PDF analysis results which showed that the C-A-S-H gel in alkali-activated binders is structurally distinct from the C-S-H product of C_3S hydration, and specifically appears more disordered[40]. If incorporation of alkali cations in the interlayer of C-A-S-H is inducing additional structural disorder, both by reducing the periodicity of the interlayer and by reducing the regularity of the stacking of the layers through differences in ionic size, this could link these nanostructural and chemical observations.

2.2 Microstructural characterisation

The most widely used tool for microstructural analysis of AAMs is scanning electron microscopy (SEM). In this context, the advances which have been made regarding analytical methods and instrumentation applied to Portland cement-based materials are also of value in the analysis of AAMs. The ability to collect hundreds or thousands of spot analyses per sample using energy-dispersive spectroscopy (EDS) via automated data collection systems is bringing vast improvements in the ability to identify, quantify and analyse specific binder components and unreacted precursors, and most of the data reduction and processing algorithms which have been demonstrated for Portland cement-based materials [44, 45] should be quite readily transferable to the analysis of alkali-activated binder systems. The higher-spatial resolution compositional analysis which is made possible by the use of transmission electron microscopy (TEM) is also of value in the analysis of the nanostructured and closely intermixed phases which coexist within alkali-activated binders, and nanoindentation may also prove to be of value in this regard [46].

Quantitative analysis of disordered phases, e.g. metakaolin and N-A-S-H gel in a low-calcium AAM, has also been demonstrated using more traditional X-ray diffraction methods coupled with the 'partial or no known crystal structure' (PONKCS) algorithm, validated and supported by SEM-EDS analysis [7], and this methodology appears to offer significant potential for future application.

As the field of alkali-activation matures as a research area, it is also becoming possible to analyse the microstructural features of relatively older samples which have been held under controlled conditions for longer periods of time. Such analysis of aged alkali-activated blast furnace slag-based samples [47, 48] has provided insight into the ongoing and cyclic nature of the alkali-activation reaction process, as the alkalis which remain in the pore solution can contribute to a very extended process of continuing reaction and microstructural development within the hardened material. In some instances (e.g. Figure 4), partial crack closure can be observed as a result of these processes, which offers interesting scope for future optimisation and development.

Preprint of: JL Provis, A Palomo, C Shi, Advances in understanding alkali-activated materials, *Cement and Concrete Research*, 78A (2015): 110-125. Final published version is available at http://dx.doi.org/10.1016/j.cemconres.2015.04.013

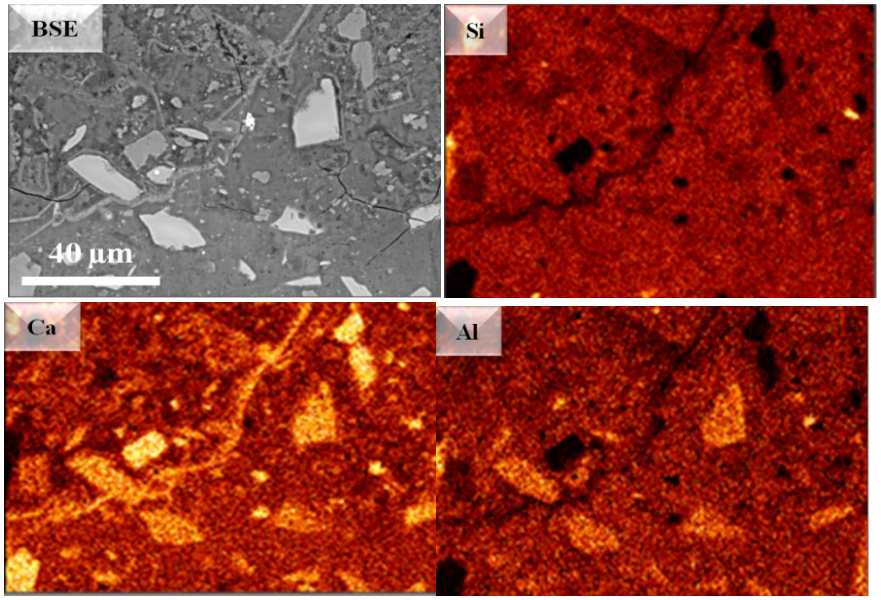

Figure 4.SEM image of the paste within a 7-year old sodium silicate-activated slag concrete, showing the deposition of calcium-rich reaction products around and inside microcracks in the paste. Reproduced from [48], copyright Elsevier B.V.

Another key tool which is gaining popularity and interest is tomography. This can be applied on both nanometre [49] and micrometre [50] length scales using X-rays, or on a nanometre scale using electrons in a transmission electron microscope [51], to provide three-dimensional insight into the geometry of the pore and solid components of AAMs.

The alkali-activation reaction process has also been better understood through rheological and surface-chemical analysis of these AAMs. The nature of the very early-age reaction products in the alkali-silicate activation of metakaolin has been elucidated through the combination of rheological measurements with small-angle scattering and other spectroscopic techniques [52-55]. Precursor particle surface chemistry has also been invoked as an explanation for the various dispersing effects, or lack thereof, achieved by the addition of polymeric dispersants to AAMs [56], as well as explaining the differing influences of silicate and hydroxide activators on the rheology of alkali-activated slag [57] and alkali-activated fly ash [58] pastes.

The electrical properties of a porous material are closely related to its pore structure and the chemical composition of pore solution, and so alternating current (AC) impedance spectroscopy provides information regarding the microstructural development during hydration of cement-based materials [59]. Figure 5(a) is a typical impedance spectrum of a cement-based material. It has a high frequency arc and a low frequency arc, characterising the bulk material effect and polarisation effect of the electrode/specimen respectively, and Figure 5(b) shows examples of the data collected for alkali-activated slag pastes at different ages. The high frequency arc in impedance spectroscopy is closely related to the microstructural characteristics of cement-based materials. Three key features, the high frequency resistance (R_1), depression angle (α) and bulk resistance (R_b), can be obtained from the spectra.

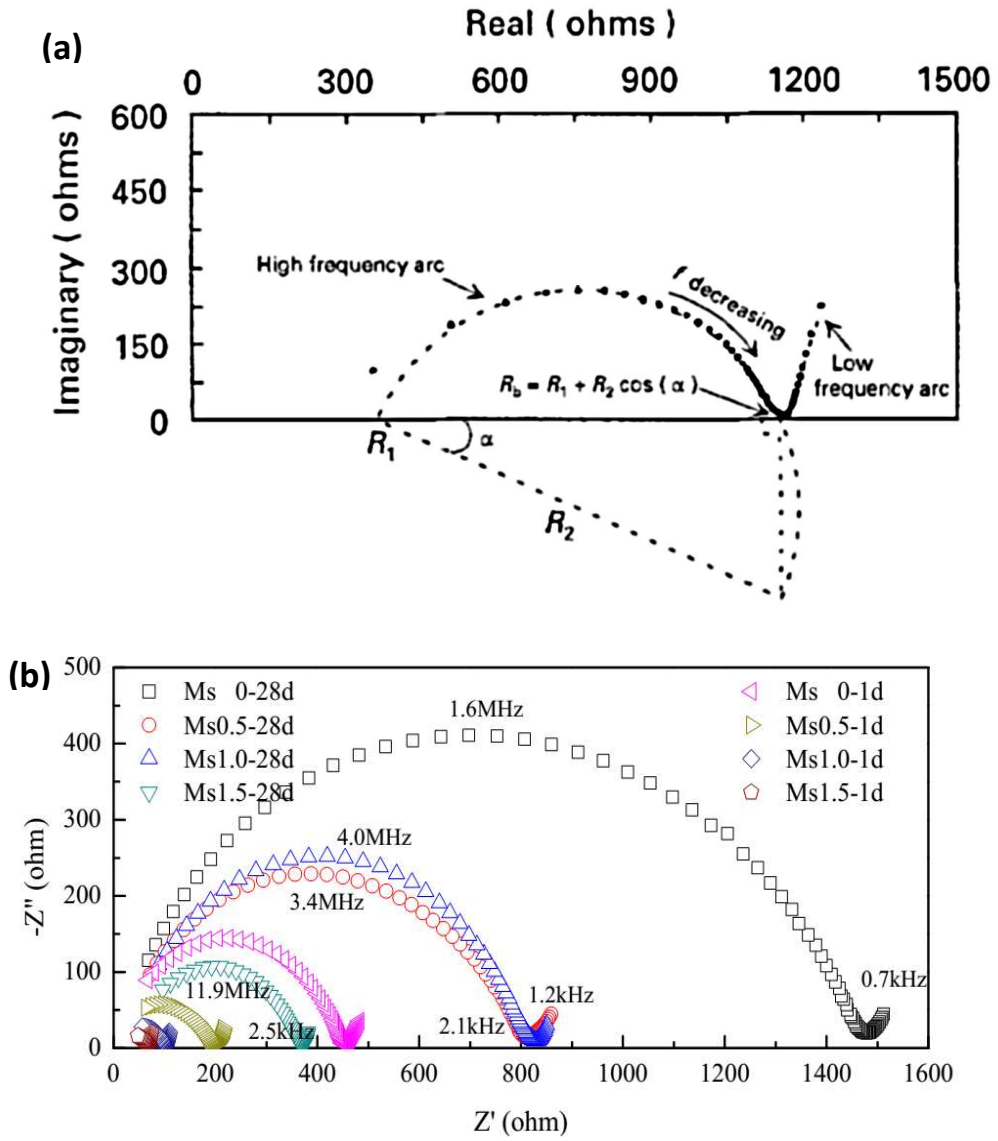

Figure 5.(a) Typical impedance spectrum of a cement-based material with key features identified; adapted from[60]; (b) impedance spectra of waterglass-activated slag with different activator moduli (Ms) at ages of 1 and 28 d; data from [61].The high frequency resistance (R_1), depression angle (α) and bulk resistance (R_b) can be obtained from the spectra; Z' and Z'' represent the real and imaginary parts of the impedance response respectively.

McCarter et al. [62] studied the early hydration kinetics of alkali-activated slag by using impedance spectroscopy over the frequency range 1-100 kHz; from the capacitance and conductance response, a number of distinct regions can be identified, corresponding to the stages of hydration, thus giving information about the chemical activity and changes in rigidity of the mixture. Hanjitsuwan et al.[63] found that the dielectric constant of alkali-activated high calcium fly ash pastes decreased substantially with increasing frequency, although this was less notable at higher NaOH concentration. The relaxation peak height decreased and the peak position shifted towards a higher frequency,

because the samples contained less unreacted fly ash and were denser than those formulated with lower NaOH concentrations.

An equivalent circuit model is an important conceptual bridge which can be used to connect the measured AC impedance spectrum with the real microstructure of the materials. Ravikumar and Neithalath [64] measured the electrical response of alkali silicate powder activated slag concretes before and after standard chloride transport tests using a proposed equivalent circuit model. They found that the resistance of the connected pores extracted from the fits of the circuit model decreased after the rapid chloride permeability test (RCPT), but increased after the non-steady state migration test (NSSMT). They ascribed this to microstructural damage imposed by the higher voltage and associated temperature increase during the RCPT, and the formation of additional chloride binding products during the NSSMT.

Liu et al. [61] proposed an equivalent circuit model to quantitatively characterize the ion concentration and pore structure of waterglass-activated slag cement during hydration. This included two parts: one describing the bulk material effect, and another to represent the electrode polarisation effects. The properties of continuous and discontinuous conductive paths, solid-solution interfaces, and interlamellar spaces between C-S-H gel could be obtained. Bulk resistance decreased with increasing dosage and modulus of waterglass due to the increase in the volume of hydration products and the decrease of ionic concentration in the pore fluid.

2.3 New modelling approaches

One rapidly growing area in cement science during the past several years is mathematical modelling of the kinetics and mechanisms of reaction during hydration, and the structure of the resulting hydrates in the hardened state[65, 66]. Puertas et al. [42] developed an atomistic structural model for C-A-S-H in alkali-activated slags using a force field-based approach, by analogy to the extensive work which has been published related to the application of this technique to C-S-H gels. Their model incorporated Na to charge-balance Al sites, and predicted crosslinking of the tobermorite chains within the C-A-S-H gel, consistent with the observation of a Q^3(1Al) site environment in the NMR spectra of many alkali-activated slag binders. To reflect this structural feature in a detailed structural chemical model for tobermorite-like C-A-S-H gels, the need for the extension of the 'substituted general model' of Richardson [67] to crosslinked tobermorite structures was identified. Myers et al. [41] provided a structurally rigorous implementation of the calculation of crosslinking degrees in tobermorite-like structures, and Richardson [68] also provided a crystal chemical model with a focus on the description of layer spacing in these gels. Models such as these are essential in enabling the correct interpretation of ^{29}Si MAS NMR spectra for C-A-S-H gels, as they provide structural constraints which may be used to guide and validate the complex process of spectral deconvolution for quantification of individual sites, thus enabling the accurate calculation of structural parameters such as Ca/(Al+Si) ratios and mean chain lengths from appropriately deconvoluted spectra [19, 69].

The description and prediction of phase assemblages through either volume-based or mass balance-based models has also become a key technique in modern cement science [70, 71], and has been applied to the study of calcium-rich AAMs [72, 73], where the coexistence of C-A-S-H phases and important secondary products such as hydrotalcite plays a major role in determining material properties including strength and durability [74]. However, uncertainty was introduced into such models by the lack of an explicit description of the roles played by alkali metals and by aluminium in the structure of the C-(N-)A-S-H gel; this has recently been resolved through the development of a

thermodynamic model entitled CNASH_ss [43] which describes this phase as an ideal solid solution between eight end-members containing different degrees of Al and alkali substitution, and gives an accurate description of solubilities in the quaternary CaO-Na_2O-Al_2O_3-SiO_2 aqueous system as well as relevant ternary (Figure 6) and binary subsystems.

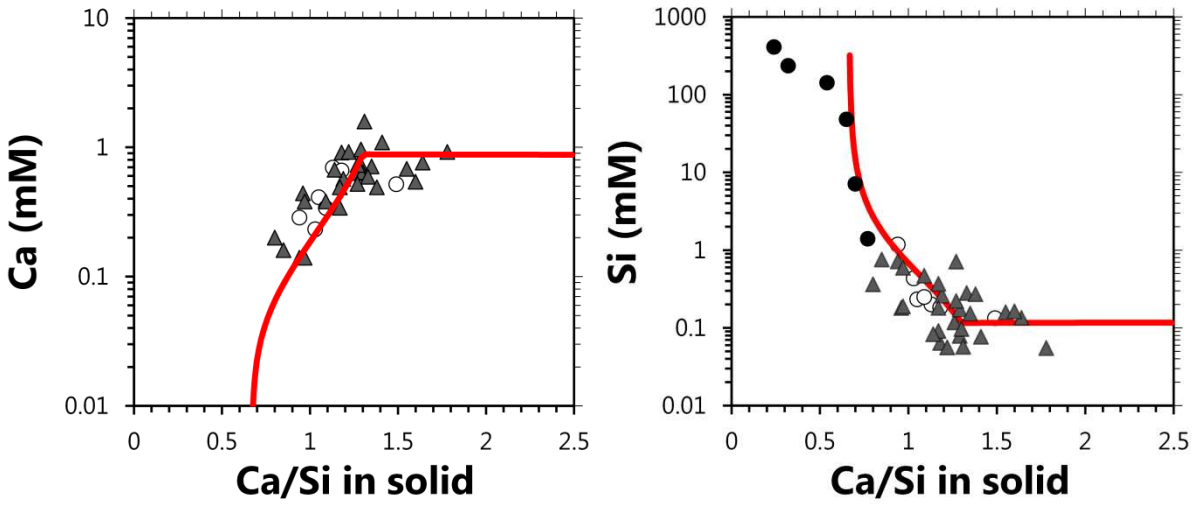

Figure 6. Comparison of CNASH_ss model predictions (lines) against experimental data (points) in the CaO-Na_2O-SiO_2 system at NaOH concentrations between 0.3-0.8 mol/L. Points of different shapes relate to different sources of data: Points marked ○ are from [75], ▲from [76], and ● from [77]. Reproduced from [43], copyright Elsevier B.V.

It is notable, however, that such models are not yet available for N-A-S-H type gels. The thermodynamics of this type of gel are less well defined, and although some work based on analogies with the thermochemistry of zeolites has begun to give promising results in describing calorimetric data [78, 79]. Šmilauer et al. have also developed a volumetric description of alkali-activated metakaolin binders based on analogies with the Powers model for water environments in Portland cement [80]. At a chemical level, probably the most promising approach to the description and simulation of N-A-S-H gels is multiscale modelling, whereby results from an atomistic simulation (e.g. using density functional theory [81, 82]) are coarse-grained and used in a larger-scale simulation such as a Monte Carlo model of gel nanostructure [83]. This has proven successful for alkali-aluminosilicate gels, but there is not yet a published multiscale model which can describe the influence of calcium on these gels, and the computational demands of this approach remain high. However, it is expected that this will be an area of continuing development in coming years, as both theoretical descriptions of AAM chemistry and available computational resources continue to improve.

3. Advances in binder development

3.1 New precursors

Early studies and applications of AAMs mainly used precursors such as blast furnace slag (BFS), fly ash, and metakaolin; the chemical and physical characteristics of these precursors, and the materials derived from them, are well described in the literature including [2, 3]. Recent studies have greatly widened the sources and types of precursors, as briefly described in this section.

3.1.1 Silico-manganese (SiMn) slag

Silico-manganese slag is a discharge from the smelting of silicomanganese. It consists of irregular porous amorphous particles, somewhat lower in calcium content than blast furnace slags, and contains a significant content (~10 wt.%) of manganese within its glassy phase. This reduces its reactivity compared to the more basic blast furnace slag. Kumar et al. [84] used sodium hydroxide as an activator for high-energy milled silico-manganese slag, and obtained alkali activated cement pastes with strength up to 101 MPa after 28 days of sealed curing at 27±2°C. However, the high-energy milling was seen to be important in achieving this performance, as the strength achieved through this process was more than three times the strength achieved through alkali-activation of the same slag processed through a regular ball-milling process.

3.1.2 Mineral processing tailings

3.1.2.1 Coal gangue

Coal gangue is a mineral waste discharged during coal excavation and washing. It is aluminosilicate in nature, and its major mineralogical components are kaolin, quartz and feldspars. The amount of coal gangue accumulated in China has already reached 3.8 billion tons; the disposal of such a large quantity of waste requires a lot of land and has caused many serious environmental problems [85]. AAMs can be prepared using calcined coal gangue with high amorphous aluminosilicate content, in combination with and chemical activators. Zhang et al. [86] found that the compressive strength of sodium silicate-activated calcined coal gangue pastes could reach 42.5 MPa after 24 h of curing at 90°C.

3.1.2.2 Red mud

Red mud, also known as bauxite residue, is a waste generated during alumina extraction from bauxite ores via the Bayer process**.** It consists mainly of SiO_2,$Al_2O_3$and Fe_2O_3, with main mineral phases of quartz, zeolites containing sodium and calcium, as well as clays, hematite, and others. All these components are suitable raw materials for AAM production[87], although sometimes thermal pretreatment is beneficial [88, 89], and red muds from highly efficient refineries which are low in Al_2O_3 tend to be relatively unreactive in alkali-activation. He et al. [90] used red mud and rice husk ash to prepare AAMs with compressive strengths of up to 20**.**5 MPa; prolonged curing significantly increased the compressive strength and Young's modulus, but reduced ductility**.**

3.1.2.3 Mine tailings

In China, more than of 87% the vanadium resources exist in hard coal**.** The tailings which remain after vanadium extraction from the coal consist mainly of quartz, feldspar, zeolites and sodium silicate [91]**.** Jiao et al. [92] activated a blend of ground vanadium tailings and fly ash with sodium silicate, with the aim of producing a fire-resistant product; the mechanical performance was retained after exposure to temperatures as high as 900°C, and no apparent microstructural damage was observed below 600°C. Zhang et al. [93] also used class F fly ash to adjust the Si/Al ratio of copper mine tailings to an appropriate level for use in alkali-activation, and used NaOH solution as the activator to prepare AAMs with appropriate physical properties for use as a regular construction material.

3.1.3 Catalyst residues

Petroleum refineries worldwide process crude oil in fluid catalytic cracking (FCC) units, and 160,000 tonnes of spent FCC catalyst residue are thus produced every year. The spent catalyst is essentially an agglomeration of zeolite (faujasite) crystals held together by an aluminosilicate matrix including amorphous silica and clays. Tashima et al.[94] studied the synthesis and mechanical

properties of geopolymer mortars produced from FCC catalyst residue, which yielded a compressive strength of about 68 MPa after 3 days of curing at 65°C. Rodríguez et al. [95] also synthesised AAM pastes using FCC catalyst residue and sodium silicate solutions to form a highly dense and crosslinked aluminosilicate type gel. However, in using this type of residue as a precursor in alkali-activation, it is important to consider the significant heavy metal content of the catalysts, particularly nickel, vanadium and/or lanthanum, as these may impact the performance of the geopolymer materials, and are also potentially leachable under some conditions. Catalysts from different sources and processes also differ in composition and reactivity, meaning that this is rather a diverse class of materials which can provide alkali-activated products with a range of performance levels [96].

3.1.4 Coal bottom ash

Coal bottom ash (CBA) is a by-product of coal combustion which is collected at the bottom of furnaces that burn coal for the generation of steam, the production of electric power, or both; fly ash is produced from the same process, but is instead captured at the top of the furnace. CBA tends to be coarser than fly ash, with grain sizes spanning from fine sand to fine gravel [97], and so needs to be milled before use in alkali-activation. It contains only a small amount of semi-spherical particles and less glass than fly ash, and so tends to result in AAMs with lower strength. However, because bottom ash is generally not accepted in Portland cement blends due to its lower reactivity and often significant heavy metal content, it is becoming popular as a potential precursor for alkali-activated binder production, at least on a laboratory scale. The morphology, particle size, surface properties, and amorphous phase content of CBAs will influence their ability to react in synthesis of alkali-activated binders. Sathonsaowaphak et al. [98] found that strengths of up to 58 MPa could be achieved when the material was ground to a sufficient fineness and combined with sodium silicate at an appropriate modulus, while Donatello et al. [99] used coal bottom ash as a high-volume component of hybrid alkaline cements.

3.1.5 Rice husk ash

Rice husk ash (RHA) is a waste generated through burning rice husk primarily for the generation of electricity or for other purposes. The main component of the ash is silica (>90–95 wt.%), existing predominantly in amorphous and partly in crystalline phases, in high-surface area particles, with residual carbon as the major impurity (depending on combustion conditions) and other trace elements such as K and Ca. The amorphous silica in RHA is reactive and can be used as a pozzolan; its use in alkali-activation requires a secondary source of aluminium, as the Al content of RHA is close to zero. Detphan and Chindaprasirt [100] used coal fly ash and RHA to prepare AAMs using NaOH and sodium silicate as activators, and found that the optimum burning temperature of RHA for making FA-RHA AAMs was 690°C. The compressive strengths ranged up to 56 MPa, depending on the ratio of FA/RHA, the RHA fineness, and the activator modulus. Bernal et al. [101] also used RHA as an alternative silica source for the production of low-cost silicate activating solutions from aqueous NaOH, which gave equivalent or better performance when compared with a commercial waterglass but with both environmental and financial benefits.

3.1.6 Palm oil fuel ash

Palm oil fuel ash (POFA) is a by-product from the palm oil industry produced in massive amounts in many parts of the world, and has particularly become of interest to researchers in south-east Asia for use as a pozzolanic additive for PC concretes as well as in alkali-activation [102]. Salih et al. [103] used POFA in combination with sodium silicate and sodium hydroxide to prepare alkali-activated binders, achieving a compressive strength of up to 32.5 MPa after 28 days of curing at 60 °C. Other

workers have also utilised POFA with other aluminosilicate materials, such as slag and rice husk ash, to make alkali-activated pastes or mortars with improved performance [104].

3.1.7 Waste glass

The recycling of waste glasses from consumer utilisation and industrial processes poses a major problem for municipalities worldwide. Tashima et al. [105] investigated the properties and microstructure of alkali-activated glass fibre waste using NaOH and KOH solution as activators. The mortar samples showed compressive strengths of up to 77 MPa after 3 days of curing at 65°Cwhen 10mol/L NaOH solution was used as activator. Balaguer Pascual et al. [106] used metakaolin (MK) to replace a part of the glass powder in order to introduce Al and also to stabilise alkali ions in the system. Compressive strength of the mortars increased with MK content up to 8%. In contrast, without MK or with less than 3% MK content, the compressive strength decreased with time**.** The need for additional aluminium sources is relatively common in the alkali-activation of waste glasses, as few commercial glass systems contain sufficient Al to produce a stable AAM.

Bajare et al. [107] investigated the use of a combination of dross from aluminium recycling, calcined kaolin clay, and lead-silica glass (LSG) from recycled fluorescent lamps, to prepare foamed alkali activated binders. The residual aluminium metal in the dross generates hydrogen when reacting with the sodium silicate activator, leading to a low-density material (460 - 550 kg/m^3), with a total porosity of 82 - 83 %, and compressive strengths from 1.1 MPa to 2.3 MPa. One of the interesting points of novelty in this work was the use of a waste material as foaming agent; this offers potential commercial and environmental benefits compared to the use of finely divided metal powders, peroxides, or surfactant-based foaming methods.

Puertas and Torres-Carrasco [108]activated blast furnace slag with three activators: commercial waterglass, a NaOH/Na_2CO_3 mixture, and the solutions resulting from dissolving waste glass in NaOH/Na_2CO_3. The compressive strength was over 60 MPa at 28 days when NaOH/Na_2CO_3 mixture and glass waste mixed solution were used as activators, indicating that this glass was potentially useful as a supplementary silica source in place of commercial silicate solutions.

3.1.8 Waste ceramic

Ceramic waste is produced in the demolition of masonry buildings, and as a by-product of porcelain and whitewares production or disposal. The ceramic waste consists mainly of SiO_2 and Al_2O_3, with the major crystalline phases of quartz (SiO_2) and albite ($NaAlSi_3O_8$), in addition to a glassy phase. A conceptual model for metakaolin could possibly be used to describe the alkali-activation of ceramic wastes, although the ceramics are usually fired at a higher temperature than is required for metakaolin formation, and so the reactivity of the material is not as high. In a study by Reig et al.[109], waste ceramics were first ultrasonically cleaned to remove contaminants such as paper scraps, metal, plastic, or other organic matter, then dried and pulverised to an average particle size (d_{50}) of around 30 µm. NaOH and sodium silicate solution were used as activators, yielding pastes with a maximum compressive strength of 41 MPa after 7 days of curing at 65°C.

3.1.9 Incineration products of sludges

3.1.9.1 Paper sludge ash

Significant residual waste streams are produced in pulp and paper mills; the solid wastes resulting from pulp production and paper mill operations are moist and contain some combustible fractions including organic wood or recycled paper fibres from which energy can be recovered (and so are

burned as recycled fuels), but also chlorinated organics, significant amounts of ash in the form of calcite and kaolinite clays, as well as trace quantities of heavy metals. Combustion of paper sludge at 700–800°C can generate an ash with a high content of highly reactive aluminosilicate components resembling metakaolin, which exhibits good pozzolanic properties [110], and can be effectively alkali-activated [111]. However, it is important to understand the composition of a paper sludge ash when using these materials in alkali-activation, as there is a very wide range of compositions among the paper sludge ashes available worldwide, ranging from materials which are mostly aluminosilicate in nature, through to some which contain mainly calcite and very little aluminosilicate material, and this must be considered carefully in any mix design process.

3.1.9.2Sludges resulting from water treatment

Reservoir sludge is comprised of the components of surface rock from a water catchment area that accumulate as loose particles aggregation at the bottom of a reservoir; this material is removed from reservoirs on a regular basis, and generally requires disposal in landfill. It is mainly composed of smectite clays such as montmorillonite. In a study [112], reservoir sludge was crushed, ground and calcined at 850°C for 6 h. A mixture of 30% blast furnace slag and 70% calcined reservoir sludge powder was activated by mixing with different alkaline solutions of water, sodium hydroxide and sodium silicate, resulting in compressive strengths of up to 63 MPa, as shown in Figure 7 .

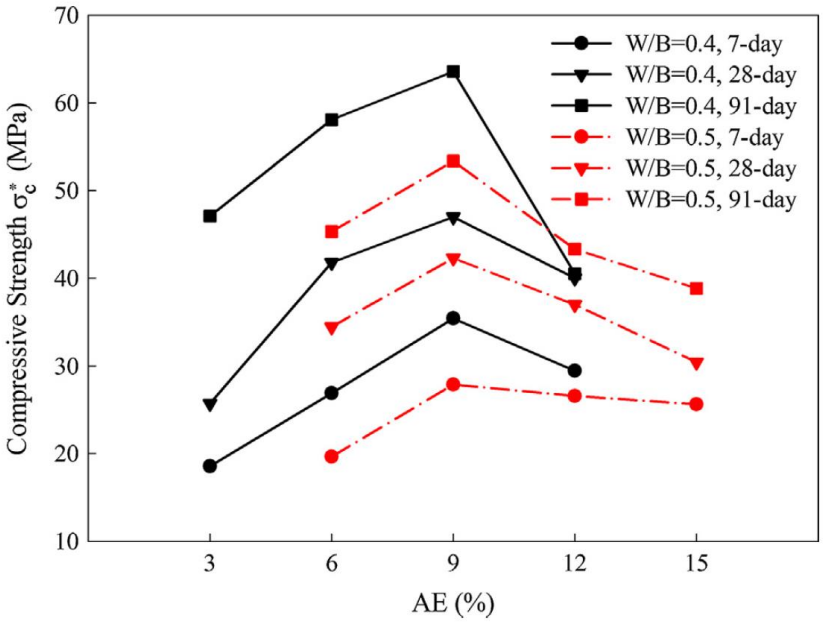

Figure 7.Effect of water/binder ratio (W/B) and Na_2O-equivalent alkali dose (AE, as a percentage of the solid powder content) on compressive strengths of alkali-activated mixtures of 30% blast furnace slag and 70% calcined reservoir sludge powder after different durations of curing at ambient temperature. From[112], copyright Elsevier B.V.

Guo et al. [113] also produced AAMs from water treatment residuals, which are a combination of the suspended solids (largely clay) removed from drinking water during its treatment, and the flocculants used to achieve its removal. Calcination of the water treatment residuals at 900°C yielded a material rich in reactive calcium, which could be blended with a fly ash-based AAM to provide improved strength.

3.1.10Natural minerals

Feng et al. [114]synthesised one-part geopolymers by thermal activation of albite with sodium hydroxide and sodium carbonate. Albite powder blended at different ratios with NaOH or Na_2CO_3 was heated at temperatures between 850 and 1150°C, then rapidly cooled to room temperature and pulverised, yielding a powder which was X-ray amorphous and highly reactive. The ground powder was added water to prepare paste samples, then cured at 25°C**.** When albite was calcined with 50% NaOH at 1000°C, the main mineral phase was identified as a disordered zeolitic/feldspathoid type compound, and the hardened paste showed a compressive strength of 44.2MPa at 28 days. There was a tendency towards efflorescence due to the very high alkali content which was used to achieve activation under such conditions, but the work does demonstrate, as a proof of concept, that the production of one-part AAMs from feldspars is possible.

Volcanic ashes, which were the original pozzolans used in Roman concretes [115], are also amenable to alkali-activation; pumice-type ashes from Iran have shown value as precursors for alkali-activated binders in combination with sodium silicate solutions, although the incorporation of a small quantity of calcium aluminate cement was found to be important in reducing efflorescence due to the low reactive alumina content of the volcanic ash [116, 117]. Cameroonian natural pozzolans have also been shown to be of value in production of both dense and porous AAMs, in studies by a number of different research groups [118-120].

3.2 Hybrid binder systems

The replacement of Portland cement with supplementary materials usually result in long setting time and lower early strength, but the addition of an extra alkali source to accelerate the reaction can result in a useful hybrid cement. Chapter 8 of reference [2] summarised previous publications on hybrid alkali-activated cements. The alkali can be supplied either via the use of a strongly alkaline solution instead of mixing water, or as a solid or dissolved Na/K compound which can react with the PC clinker to generate alkalinity *in situ*.

The reactivity of fly ash in hybrid alkaline cements is much faster than in the absence of added alkalis, depending on the reaction conditions, particle shape, mineralogy and granulometry. The reactivity of fly ash increases with increasing vitreous content [121]and the reduction of particle size[122, 123], as well as with increasing alkalinity generated by the activator. Garcia Lodeiro et al. [124] analysed hybrid cements activated with solutions of different alkalinity, and found that while the type of alkaline activator impacted reaction kinetics and the formation of secondary reaction products (particularly carbonates and AF_m phases), it did not appear to have any material effect on the nature of the main cementitious gels formed. The thermodynamically stable majority product was a mix of cementitious gels that formed irrespective of the activator used; however, the proportions of these gels will be significantly affected by the type of activator. While a highly concentrated alkali promotes the reaction of the fly ash and the precipitation of a (N,C)-A-S-H type gel, the use of activators of moderate alkalinity favours the formation of C-A-S-H type gels [124]. Bernal et al. [125] also showed that the combination of Na_2SO_4 with calcined clays, white Portland cement and limestone results in a mixture of AFm, AFt, C-A-S-H and N-A-S-H phases in varying proportions depending on the mix design.

Sanchez Herrero et al. [126, 127] have provided evidence for different mechanisms of hydration of calcium aluminates and calcium silicates depending on the pH of the medium (higher than 12-13) and

on the ionic species involved in the hydration reactions. The presence of either Na_2SO_4 or Na_2CO_3 improves the mechanical strength development of synthetic tricalcium aluminate by favouring calcium carboaluminate (from Na_2CO_3) or sulfoaluminate (from Na_2SO_4) formation. Carboaluminate formation is favoured over the precipitation of cubic and hexagonal hydrates. Na_2SO_4 stimulates the formation of the U-phase[128], which, being morphologically similar to calcium monosulfoaluminate, contributes to strength development in the matrix by densifying the material. Hydrating both C_3S and C_2S with an 8 M solution of NaOH favours the precipitation of portlandite, leading to more rapid hydration and a higher degree of reaction in both C_3S and C_2S, but particularly the latter [129]. Given the low initial activity of C_2S under normal hydration, this finding has implications for the possible creation of a new family of belite cements. It was also demonstrated that the non-hydraulic polymorph γ-C_2S can be alkali-activated [130, 131], which offers further scope for developments in C_2S-based cements.

Fernández-Jiménez et al. [132]also demonstrated the use of solid Na_2CO_3 and K_2CO_3 as activators to obtain a hybrid cement from a blend of 20 % clinker + 40 % blast furnace slag + 40 % metakaolin. The use of solid carbonate activators is very attractive from a commercial perspective as these are less expensive to procure, and much less difficult to handle, than aqueous silicate or hydroxide solutions. The highest mechanical strength values were obtained with 5 % Na_2CO_3 as activator, which yielded a mix of (N,C)-A-S-H and C-A-S-H cementitious gels as the main reaction products, along with metastable calcium monocarboaluminate, which later evolved into the calcite or vaterite forms of calcium carbonate.

Arbi et al. [133] combined blast furnace slag or diatomite with an alkaline activator in the presence of reactive aluminium sourced from calcium aluminate cement (CAC). The main reaction product was a cementitious gel that precipitated with crystalline phases such as ettringite, the U-phase, and katoite. While the slag-blended binder reacted to generate a C–(A)–S–H-like gel under moderately alkaline conditions, diatomite reactivity proved to be very low under such conditions. The greater reactivity of both slag and diatomite at high pH (high alkalinity) favoured their interaction with CAC.

4. Advances in durability

4.1 Durability and thermodynamics

The countless examples in nature of the presence of alkalis, and particularly of alkaline aluminosilicates, in rocks stand as geological and consequently thermodynamic proof that these compounds, appropriately proportioned and combined with network-forming elements, are highly stable (insoluble). Moreover, the temperatures and pressures needed to manufacture AAMs are similar to the conditions prevailing in some of the processes involved in sedimentary rock formation. Residual soils often contain low-temperature forming sedimentary zeolites such as phillipsite [$(K_2,Ca)Al_2SiO_{12}.4.5\ H_2O$], scolecite [$CaAl_2Si_3O_{10}.2H_2O$], analcime [$NaAlSi_2O_6.H_2O$], mordenite [$(Ca,Na_2,K_2)Al_2Si_9O_{22}.6H_2O$] or natrolite [$Na_2Al_2Si_3O_{10}.2H_2O$] [134, 135].

Analcime, for instance, tends to form on certain temperate seabeds (temperatures of under 30 °C), an outcome of the interaction between volcanic ash and alkaline metals dissolved in the seawater. The sole determinants of its formation, and that of other zeolites, are the concentration of the elements in the seawater in contact with the ash, and the water temperature. While in high calcium

media, calcium-bearing zeolites are the varieties most prone to precipitation, when the alkali concentration is high, sodium or potassium partially or wholly replace the alkaline-earth cations [135]. The result is an alkaline metal-rich precipitate, which is entirely compatible with the presence of alkaline-earth metal zeolites.

Resistance to decay is clearly more effective in alkaline aluminosilicate hydrates such as muscovite and paragonite than in calcium aluminosilicates. The existence of these sodium- and potassium-bearing minerals in nature further supports the excellent durability of compounds similar to the products of alkaline activation. Krivenko et al. [3, 136] built a flowchart of sedimentary rock formation from the products of rock weathering, which was then used as a basis for modelling artificial minerals.

Processes such as silicate condensation and polymerisation, then, with the attendant changes in the respective mineral phases, all exhaustively studied under laboratory conditions, also take place in the Earth's crust. That would appear to constitute irrefutable evidence of the thermodynamic stability of the reaction products, and provides positive indications regarding the long-term durability of AAMs.

4.2 Testing for durability

Most previous studies have focused on the process of alkali activation and mechanical properties of alkali-activated cements and concretes, with less emphasis on durability aspects until recently. A host of standards with respect to durability testing have been well established and widely applied to Portland cement concretes, but their applicability for AAMs remains to be addressed. The two books [2, 3] summarise previous studies on durability of AAMs; this section outlines some recent relevant publications and presents some important arguments with respect to durability testing of AAMs.

4.2.1 Chloride ingress and binding

Chloride ingress and binding in concrete are very important in defining the time taken to initiate corrosion of steel in reinforced concrete structures and elements. Douglas et al. [137] used the RCPT method to measure the charge passed by alkali-activated slag cement concretes, and obtained results corresponding to the values expected for a low water/cement ratio Portland cement concrete. Mercury intrusion measurement of corresponding mortar specimens indicated that Na_2SiO_3-activated slag mortars exhibited much lower porosity and finer pore structure than Na_2CO_3-activated and NaOH-activated slag mortars. However, the RCPT results indicated that Na_2SiO_3-activated slag mortars exhibited a much higher charge passed, particularly at early age, while those activated by NaOH or Na_2CO_3 showed little change in charge passed from 3 to 90 days. It is speculated that the chemistry of the pore solution appears to contribute more to the electrical conductivity or the charge passed than does the pore structure, for alkali-activated slag cement mortars and concretes. These problems become much more severe when different AAMs are compared[3]. Bernal et al. [138] studied the resistance of alkali-activated concretes to chloride permeability by RCPT and direct diffusion tests, and found that the correlations between the chloride diffusion coefficient resulting from the two methods were weak, which further reveals the limitations of the RCPT in analysis of alkali-activated concretes. It seems that the nature of the alkali-activated gel hydration products strongly influences chloride ionic transport [139], but a full description of these processes has not yet been published. In high-Ca alkali-activated systems, the C-A-S-H reduces porosity, while in low-Ca systems the N-A-S-H, which is more porous[50], appears to contribute significantly to higher chloride binding [139].

The RCPT method is based on the measurement of electrical conductivity, which determined by

both pore structure and solution chemistry. Thereby the results from this method may be misleading if the pore chemistry becomes dominant in the measurement [140]. The pore chemistry becomes more complicated due to the addition of an alkali activator, which can buffer the pore chemistry at very high pH during hydration [141]. So, it has become attractive to apply alternative accelerated chloride migration tests such as the NordTest method NT Build 492[142], or ponding tests such as ASTM C1543 [143], which use the colour change induced by application of silver nitrate solution to a split sample surface to determine the chloride penetration depth, and thus chloride diffusion coefficients. Such tests provide a more evident correlation to field performance because chloride movement is measured directly. However, it should be noted that the alkalinity and volume of pore solution of cement-based materials, and the concentration and volume of sprayed $AgNO_3$ solution all influence the chloride concentration at the colour change boundary in the silver nitrate colorimetric method [144, 145]. This may cause some variation in the test results [146], particularly for AAMs.

4.2.2 Carbonation

Carbonation of cements through uptake of CO_2 from the atmosphere causes a decrease in the alkalinity of concrete, increasing the susceptibility to corrosion of steel reinforcement. This depassivation of the steel in alkali-activated concretes can take place either directly due to reduced pH [147, 148], or coupled with chloride attack [149]. The mechanism of carbonation in AAMs is obviously different from that which takes place in Portland cement[150]. In Portland cement pastes, atmospheric CO_2 dissolves in the pore solution and reacts rapidly with portlandite to form$CaCO_3$, and then with C–S–H gel to form $CaCO_3$ and silica gel[151].In contrast, the carbonation of alkali-activated slag paste occurs directly in the C–A-S–H gel because of the lack of portlandite, leaving an alumina-containing remnant siliceous gel in addition to $CaCO_3$ [18, 152]. Carbonation can also induce a loss of strength and an increase in pore volume in alkali-activated concretes [153]. The hydrotalcite-group phases produced as a secondary product in most alkali-activated slag binders are also observed to play a significant role in binding carbonate ions and retarding the progress of carbonation [74].The carbonation of low-calcium alkali-activated binders appears mainly to involve conversion of the alkali-rich pore solution to carbonate or bicarbonate salts [154], with little nanostructural alteration identifiable in the binder gel itself (as the N-A-S-H gel cannot undergo decalcification processes)[18], but the mechanisms of strength loss induced by carbonation of such materials still require further investigation.

Another key determining factor for carbonation processes is relative humidity (RH), where an intermediate humidity is required to enable uptake of CO_2 from the atmosphere, which is slow under either very dry or saturated conditions. Most accelerated carbonation tests use relative humidities between 50-70% [155], where the majority of concretes (including alkali-activated slags) are carbonated at the fastest rate [156]. However, exposure of immature samples to lower relative humidities during accelerated carbonation tests can result in significant drying shrinkage, and subsequently induce microcracks [156], which certainly contributes to the rapid carbonation of AAMs in accelerated tests.

A complication in this discussion is that accelerated carbonation testing of alkali-activated binders, carried out at elevated CO_2 concentrations, has been shown to provide results which are unlikely to represent the behaviour of the products under actual service conditions, due to changes in alkali carbonate phase equilibria when the CO_2 concentration is increased [153, 157]; the tests are highly aggressive to alkali-activated binders, meaning that assessment based on test results may overestimate the risk of carbonation of these materials in the field. Under natural CO_2 conditions, the

636 excess alkalis present in the pore solution of an alkali-activated binder will quite possibly maintain the
637 internal pH at a level which is sufficiently high to protect steel in a passive state [157]. Carbonation at
638 early age is expected to reduce the achievable extent of reaction by limiting the availability of alkalis,
639 and extremely high pH, which are needed for the reaction process to continue, and so this may be
640 damaging to the performance of the material. The influence of carbonation on the mechanical
641 integrity of the binder phases also needs to be examined, as there are indications that a loss of
642 strength may take place during carbonation [138], but the mechanisms involved in this change in
643 mechanical performance still require further investigation. Given that the currently testing methods
644 are excessively aggressive, but a relatively high degree of acceleration is required to make the slow
645 natural carbonation processes observable on a laboratory timescale, how can an appropriate and
646 reliable test be designed and implemented? This also requires further attention.

647 ### 4.2.3 Sulfate attack

648 Deterioration of concrete due to sulfate attack is generally attributed to reactions of calcium-rich
649 cement hydration products with sulfates to form expansive reaction products after hardening, which
650 produces internal stress and a subsequent expansive disruption of the concrete[158]. Due to differences
651 in phase chemistry of the hydration products, and specifically the absence or low concentrations of
652 AFm phases in AAMs, the mechanisms of sulfate attack observed in alkali-activated concrete are
653 notably different from those in Portland cement. Shi et al. [2] and RILEM TC 224-AAM [3]summarised
654 earlier research on the sulfate attack resistance of alkali-activated slag; the conclusion was that AAMs
655 appear to be superior to regular Portland cement under exposure to most sulfate solutions, and even
656 superior to sulfate-resistant Portland cement when exposed to sodium sulfate solutions. This particular
657 aspect of the performance of AAMs is brought about because Na_2SO_4 can actually be used as an
658 activator in higher-Ca AAMs [159], and thus would favour the structural evolution of the binding
659 phases and densification of the system [2]. However, when AAMs containing any significant level of
660 calcium are immersed in $MgSO_4$ solutions, significant loss of compressive strength occurs due to
661 decalcification of the C-A-S-H, gypsum and/or ettringite can be formed [160-162].There has been little
662 detailed investigation of the sulfate resistance of calcium-free alkali-activated binders, as the
663 expansive processes which take place in calcium-rich materials are unlikely to be replicated in the
664 absence of significant contents of calcium in the binder.

665 The other important aspect of the interaction between cementitious materials and sulfates is
666 related to internal sulfate attack, whereby sulfates included in the original mix can cause expansive
667 processes at later ages. This is of particular interest in the context of nuclear waste immobilisation,
668 where different methodologies including direct incorporation of sulfates into metakaolin-based
669 binders [163], and the use of $Ba(OH)_2$ as an additive in slag-based binders containing Na_2SO_4, to
670 simultaneously bind sulfate as $BaSO_4$ and generate alkalinity for slag activation [164], have recently
671 been demonstrated.

672 ### 4.2.4 Acid Attack

673 Hydrated cement paste is an alkaline material and can be attacked by acidic solutions, where the
674 removal of calcium leads to structural damage and loss of performance. Many studies have
675 demonstrated that AAMs can show better acid corrosion resistance than Portland cement pastes due
676 to the differences in the nature of their hydration products. The dissolution of $Ca(OH)_2$ and calcium
677 sulfoaluminates from Portland cement, and the decalcification of high Ca/Si ratio C-S-H, either leaves
678 a very porous corroded layer or simply removes the specimen surface. Conversely, the low initial
679 permeability of alkali-activated slag specimens, along with the low CaO/SiO_2 ratio typical of the C-A-S-

H in such binders, leaves a coherent layer of aluminosilicate gel even after decalcification [165, 166]. This can hinder the further ingress of acids, contributing to the high acid resistance of AAMs [166, 167]. Pu et al. [168] also noted that for AAMs based on different slags, the less-basic slags yielded binders with better acid resistance.

Corroded depth and mass loss are often used to characterise the acid induced degradation of cements and concretes. Lloyd et al. [166] found that the corroded depth was a more sensitive measurement of the progress of attack on AAMs than change in mass, because acid attack on N-A-S-H gels leads to the formation of an apparently intact, but porous and low-strength, reaction product layer on the sample surface, rather than actual dissolution of the binder. Shi and Stegemann [169] found that the corroded depth of alkali-activated slag paste was about 1.3 mm, compared to 2.5 mm for Portland cement paste after 580 days of immersion in pH 3 nitric acid solutions, and its resistance to corrosion in HCl and H_2SO_4 was also higher than that of Portland cement paste[169]. However, the dealumination of N-A-S-H gel has been identified in HCl solution, along with the destruction of the zeolites formed in alkali-activated fly ash binders, independent of the type of activator used [170].

4.2.5 Alkali-aggregate reactions

As was mentioned in section 4.1, AAMs usually contain a very high content of alkalis, meaning that potential alkali-aggregate reactions (AAR) become a concern in infrastructure applications [171]. Based on the relationships between alkali-silica reaction expansion and slag content of Portland-slag cement, it seemed that deleterious expansion would not happen when the slag content was higher than 80% and alkali content over 4%[2, 172]. It has been argued that this is because replacement of Portland cement with high volume blast furnace slag and/or fly ash will result in C-S-H with a low Ca/Si ratio and significant Al content, that can bind more alkali ions than that with a higher Ca/Si ratio, and so inhibit AAR [172]. Many researchers have confirmed that AAR does in fact happen in alkali-activated slag-based materials [173-176], with significant amounts of AAR reaction product observable under electron microscopy [176], but the expansion was in almost all cases smaller than that of conventional Portland cement-based materials tested in parallel. Among these studies, a trend was identified that as the replacement of blast furnace slag with low calcium fly ash or metakaolin in an alkali-activated binder increased, the expansion of the specimens decreased, and alkali-activated fly ash or metakaolin materials, even with alkali-reactive aggregates, demonstrated very small or negligible expansion [175, 177, 178]. The low availability of calcium in the pore solution of the alkali-activated binders is also likely to contribute to restricting the expansive processes [179], as is the binding of pore solution alkalis by incorporation into aluminosilicate reaction products.

The accelerated mortar bar test method (ASTM C1260 [180]) has been most widely used for screening alkali-reactive aggregates and evaluating the effectiveness of supplementary cementing materials in supressing AAR. In this testing procedure, the mortar bars are cured for only 24 h, then submerged in water for 24 h, and afterwards in 1 M NaOH solution at 80°C. Immersion in water at such early age can result in a severe problem for AAMs, as the leaching of alkalis is damaging to the maturity development of the binder [3]. Thus, AAM mortars are often cured in steam, rather than in water at 80°C, before immersion in NaOH solution, but this does render the test strictly non-compliant with the ASTM standard. Another consideration is that the alkali concentration in the immersion solution, 1 M NaOH, is designed to test AAR in Portland cement mortars, but is lower than the intrinsic alkali content of most alkali-activated binders [181], and thus the contribution of the external alkalis may actually be very limited. Also, expansion measurement of the mortars in this test starts only 48 h after mixing, when the binders, especially with low calcium aluminosilicate glass precursors, are not

yet well hydrated. This might be problematic since a significant overlap of chemical shrinkage and AAR expansion could take place, resulting in a reduced or non-observable expansion of the specimens [182].

Shi [2, 183] also used an autoclave method to examine the alkali-silica reaction in alkali-activated phosphorus slag cement, but found that this test was not suitable because the alkali aggregate reaction might happen before the raw material was fully activated. Thus, both the AAR mechanisms and testing methods need further detailed studies.

4.3 Predicting durability

The prediction of in-service performance, and specifically service life, of a reinforced concrete element based on laboratory test results remains essentially a 'holy grail' for much of the field of cement and concrete science. There are relatively well-defined approaches to this problem for plain Portland cement concretes, where a suite of largely validated testing methodologies are used to obtain information regarding the physicochemical characteristics of concretes, and these characteristics are then used as the inputs of predictive models based on given exposure conditions, cover depths and other parameters. For AAMs where, as was noted above, the applicability of various testing methods for Portland cement is questionable at best [3], such an approach is prone to errors [4]. The interactions between different degradation mechanisms, e.g. binder carbonation and chloride corrosion of steel, are likely to differ between alkali-activated and Portland cement binders [147, 157], but there is still a significant degree of work required to fully understand and validate the description of these interactions.

5. Advances in processing

Alkaline activation, from its rapid upswing in popularity in the scientific and technical scene since the 1990s, has experienced a very high level of scientific advancement; the quantity and the quality of fundamental knowledge generated in the last decades around the materials synthesised by alkaline activation is notable. Many interesting concepts supported by the chemistry of alkali activation of aluminosilicates have opened up a range of possibilities for the development of new materials: electronic composites with carbon nanotubes, photoactive composites with oxide nanoparticles, bioactive materials, drug delivery agents, dye carrying media, novel chromatography media, precursors for oxide or non-oxide ceramics, fluorescent materials, novel catalysts, solid-state hydrogen storage media, nanoporous materials, fibre-reinforced composites, and others [184].

Production of alkaline concrete, which has already been successfully applied with slag-based mixtures in the second half of the 20th century [185] and with fly ash-based mixtures from the beginning of the 21st century [186],has evolved over time based on objectives of 'sustainability' (maximum use of industrial waste), 'economy' (concrete cheaper than Portland cement concrete) and 'durability'. The preparation of ready-mixed or precast concrete using alkaline formulations is probably the processing technology in the field of the alkaline activation which has developed most rapidly in the last few years.

Heat treatment has also opened new possibilities of alkaline activation in relation to new products. For example, high-purity leucite [187]and pollucite [188] have been prepared by heating metakaolin-based geopolymers, containing potassium and caesium respectively, and with designed Si/Al ratios. These are technologically valuable ceramics, leucite as a dental material, and pollucite

because of its low thermal expansivity. Kuenzel et al. [189] transformed metakaolin-based AAM mortars into polycrystalline nepheline/quartz ceramics with relatively high compressive strength (~275 MPa) and high Vickers hardness (~350 HV). The application of appropriate thermal treatments or chemical admixtures can also lead to special products such as lightweight cements or foams [190-192].

The manufacture of bricks for construction has also been the object of attention in the field of alkali activation; in Malaysia [193], the USA [194] and India [195], various brick-making processes have been adapted to the use of alkali-activated binders instead of firing bricks in a kiln.

6. Quantification of sustainability

The raw materials related to Portland cement, such as limestone and clay, are non-renewable resources. The production of one tonne of Portland cement consumes 3-6 GJ of energy and releases about 0.85 tons of CO_2 [196]. The precursors of AAM are mainly industrial byproducts or wastes. Some of them can be used directly, some of them may need grinding and some of them may need calcination or thermal activation at 700-900°C. Thus, it has been identified that AAMs should have advantages in sustainable development over conventional Portland cement, even when the emissions associated with the production of the activator are taken into consideration.

Many of the published studies which aim to assess the environmental footprint of AAMs attempt to take a holistic view on a worldwide (or continent-wide) basis – but in doing so, any opportunities for precision in terms of describing the actual production, transport and utilisation of specific materials in a given location, are lost. It is precisely this level of detail which is required, if a meaningful comparison with currently-used technologies is to be drawn. For this reason, any broad statement that AAMs offer the possibility to save a certain percentage of CO_2 emissions compared to 'Portland cement' is prone to inaccuracy, unless the full system is precisely specified: the location, the source of every material component, the functional unit (whether this is defined by volume of concrete, mass of paste, normalised to compressive or flexural strength, or by some other method), the mix design of the alkali-activated material, and the mix design of the reference Portland cement mix (based on the understanding that different blended cements now dominate the market in many parts of the world, and in some places the use of a non-blended Portland cement in concrete production is becoming rather unusual). When this is done with care, e.g. [197-199], valuable results can be obtained, but there is still a strong need for further, detailed, comparative life-cycle studies of alkali-activated and Portland cement-based concretes, based on validated input and inventory data, and in specific locations to account accurately for energy generation mixes, supply-chain and transport considerations. It is only through the availability of such information that the environmental performance of AAMs can be accurately assessed, and the current status of research in this area does not yet in general provide the necessary level of specificity.

It has been identified that the most critical factor determining the environmental footprint of an alkali-activated concrete is the activator dose, particularly when silicate or hydroxide activators are used [200]; this is also likely to be the most expensive component of any alkali-activated concrete mix, which means that a producer has dual incentives to design an efficient mix design with minimal activator content. Habert et al. [199] used life cycle assesment methodology to analyse the environmental impacts of AAM concretes made with fly ash, blast furnace slag and metakaolin based on published results. A calculation based on an average of 49 mix designs published in the scientific

literature (and thus produced without the intention to minimise either cost or environmental footprint) indicated that fly ash based geopolymer mixtures released 45% less CO_2 than an average Portland cement concrete mixture. Granulated blast furnace slag based binders showed lower emissions, but metakaolin-based geopolymer showed higher global warming effects than Portland cement, due to the high activator doses used in such mixes in most laboratory studies. Additionally, calcination of metakaolin at 800°C consumes around 50% of the energy, and generates about 33% of the CO_2 emissions, compared to the production of Portland cement [201]. Figure 8, derived from the work of McLellan et al. [198], exemplifies the importance of the activator in the emissions calculations for several fly ash-based AAM formulations; the vast majority of the emissions are attributed to the activator component, while the transport of the fly ash is also a significant contributor in the context of that country. This highlights the importance of efficient and economic mix design in ensuring the environmental credentials of any particular alkali-activated binder system: these materials are not intrinsically or fundamentally 'low-CO_2' unless designed effectively to achieve such performance, but when mix design and raw materials selection are carried out with a view towards optimisation of environmental performance, the outcomes can result in very significant savings.

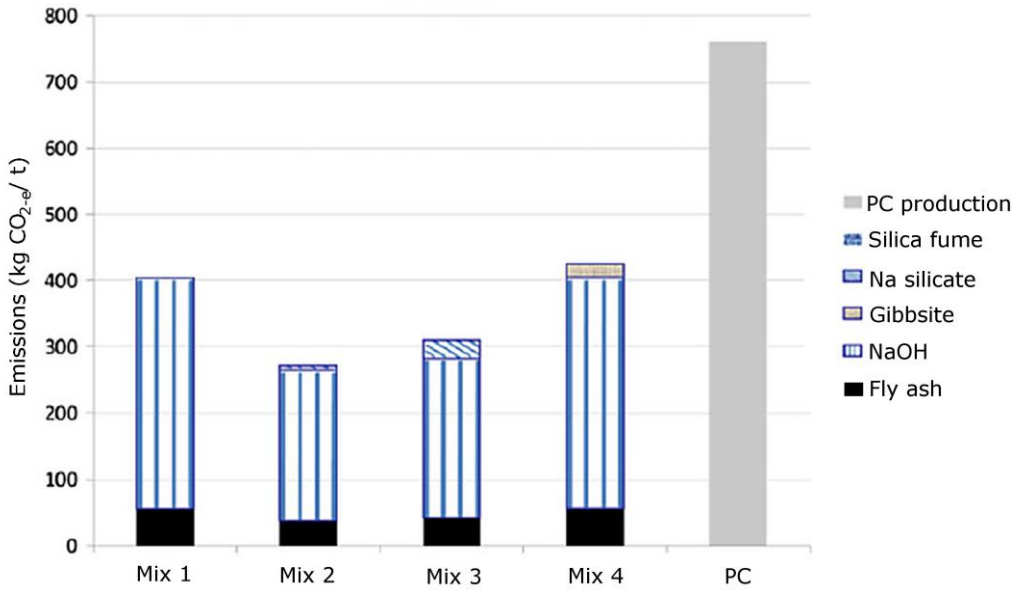

Figure 8. Calculated CO_2-equivalent emissions of four different fly ash-based AAM paste mix designs, each with target strength 40 MPa, compared to a typical Portland cement, incorporating transport and electricity emissions calculated using typical Australian data. Adapted from [198].

7. Conclusions and perspectives

The development and use of AAMs as an alternative to Portland cement-based materials for construction and other applications, has advanced extremely rapidly in the past several years. These materials are now deployed on a commercial scale in multiple nations around the world, in infrastructure, general construction and paving, nuclear waste immobilisation, and various other niche applications. Hybrid binder formulations, making use of concepts and components from both alkali-activation and Portland cement chemistry, are also becoming appealing due to their potential to offer a more robust and less expensive pathway to AAMs.

The science required to underpin the large-scale utilisation of this class of materials has been developed based on both bottom-up and top-down analytical procedures and design protocols. There are still a number of areas which require attention, from both scientific and technological perspectives, and particularly including the control of setting time and rheology. The development and optimisation of alkali-activated binder formulations from an increasingly diverse range of waste-derived precursors has become the focus of efforts from many research teams worldwide, often with a focus on locally-available or problematic materials. This diversification both highlights the versatility of the alkali-activation process, and also raises significant scientific questions related to materials characterisation and optimisation, which would be required for legislative acceptance and standardisation of the AAMs produced in this way. Appropriate and meaningful testing and description of both durability and environmental sustainability is essential in ensuring the future role of alkali-activated binder systems in the future global construction industry, and advanced processing methodologies will be of value in enabling the true value of this class of materials to be unlocked and realised.

It is also essential to develop AAM formulations, and new activators (sole components or combinations) which provide desirable early- and late-age properties, while minimising the environmental footprint of the material as a whole. The large-scale utilisation of commercially-produced sodium silicate as an activator will face limitations in terms of scalability, cost, practical handling issues and the environmental cost of this product. Thus, it is essential to develop appropriate alternatives. Advances in the development of processing routes which enable the more efficient use of activators with reduced doses for equivalent performance will also be important.

The scientific and technological maturity of the field of alkali-activation is rapidly increasing. These materials are now genuinely moving from the laboratory into the field, and generating opportunities for improvements in environmental sustainability and engineering performance (and thus also profit) which are attracting the interest and support of industry, specifiers and regulatory authorities worldwide. Some key aspects require detailed research attention in future years:

- Defining in detail the links between the physicochemical properties of complex precursors, selected activators, and the performance of the resulting binder. recommendations for improved characterisation of the precursor materials themselves, which are mineralogically complex, heterogeneous, and often span a broad range of particle sizes and shapes;
- to seek new information through the use of analytical tools which have been under-utilised, or not used at all, in the study of AAMs (e.g. Raman spectroscopy, confocal microscopy, X-ray photoelectron spectroscopy);
- development of selective chemical attack methods for the separation of phases and remnant precursors, and accurate quantification of the extent of reaction of aluminosilicate precursors in AAMs;
- to synthesise pure products from chemical reagents, simulating the chemistry of ‘real’ alkali-activated binder gels, to enable characterisation and comparison between pure products and geopolymers from real precursors, and understanding of the structural and chemical effects of minor elements;
- new activators should be investigated in order to contribute to fabrication of inexpensive binder systems, sustainable processes, and non-hazardous handling;
- methods for the characterisation of particle surface chemistry under high ionic strength, chemically aggressive conditions prevailing within AAMs;

- the thermodynamic description of N-A-S-H gel for its incorporation into geochemical-type models;
- identification and modelling of rheological characteristics of alkali activated pastes and concretes, including the effects of different families of chemical additives on the rheological properties: new water reducers, shrinkage controllers, foaming agents, and others;
- characterisation of transitional zones between aggregate-paste or reinforcement-paste within AAMs.

8. Acknowledgements

The contributions of JLP were supported by the European Research Council 7th Framework Programme, through the Starting Grant "GeopolyConc" (StG-335928), those of C. Shi were supported by National Science Foundation of China under contract Nos. U1305243 and 51378196. The authors thank Dr Susan Bernal, Rupert Myers and Dr Claire White for providing graphics.

9. References

[1] C. Shi, A. Fernández-Jiménez, A. Palomo, New cements for the 21st century: The pursuit of an alternative to Portland cement, Cem Concr Res, 41 (2011) 750-763.

[2] C. Shi, P.V. Krivenko, D.M. Roy, Alkali-Activated Cements and Concretes, Taylor & Francis, Abingdon, UK, 2006.

[3] J.L. Provis, J.S.J. van Deventer (ed.), Alkali-Activated Materials: State-of-the-Art Report, RILEM TC 224-AAM, Springer/RILEM, Dordrecht, 2014.

[4] S.A. Bernal, J.L. Provis, Durability of alkali-activated materials: progress and perspectives, J Am Ceram Soc, 97 (2014) 997-1008.

[5] J.L. Provis, S.A. Bernal, Geopolymers and related alkali-activated materials, Annu Rev Mater Res, 44 (2014) 299-327.

[6] A. Palomo, P. Krivenko, I. Garcia-Lodeiro, E. Kavalerova, O. Maltseva, A. Fernández-Jiménez, A review on alkaline activation: new analytical perspectives, Mater Constr, 64 (2014), article e022, doi:10.3989/mc.2014.00314.

[7] R.P. Williams, R.D. Hart, A. van Riessen, Quantification of the extent of reaction of metakaolin-based geopolymers using X-ray diffraction, scanning electron microscopy, and energy-dispersive spectroscopy, J Am Ceram Soc, 94 (2011) 2663-2670.

[8] G. Le Saoût, M. Ben Haha, F. Winnefeld, B. Lothenbach, Hydration degree of alkali-activated slags: A ^{29}Si NMR study, J Am Ceram Soc, 94 (2011) 4541-4547.

[9] I.G. Richardson, A.R. Brough, G.W. Groves, C.M. Dobson, The characterization of hardened alkali-activated blast-furnace slag pastes and the nature of the calcium silicate hydrate (C-S-H) paste, Cem Concr Res, 24 (1994) 813-829.

[10] J.L. Provis, G.C. Lukey, J.S.J. van Deventer, Do geopolymers actually contain nanocrystalline zeolites? - A reexamination of existing results, Chem Mater, 17 (2005) 3075-3085.

[11] A. Palomo, F.P. Glasser, Chemically-bonded cementitious materials based on metakaolin, Br Ceram Trans J, 91 (1992) 107-112.

[12] S.A. Bernal, E.D. Rodríguez, R. Mejía de Gutierrez, M. Gordillo, J.L. Provis, Mechanical and thermal characterisation of geopolymers based on silicate-activated metakaolin/slag blends, J Mater Sci, 46 (2011) 5477-5486.

[13] I. Ismail, S.A. Bernal, J.L. Provis, R. San Nicolas, S. Hamdan, J.S.J. van Deventer, Modification of phase evolution in alkali-activated blast furnace slag by the incorporation of fly ash, Cem Concr Compos, 45 (2014) 125-135.

[14] C.K. Yip, G.C. Lukey, J.S.J. van Deventer, The coexistence of geopolymeric gel and calcium silicate hydrate at the early stage of alkaline activation, Cem Concr Res, 35 (2005) 1688-1697.

[15] E.M. Gartner, D.E. Macphee, A physico-chemical basis for novel cementitious binders, Cem Concr Res, 41 (2011) 736-749.

[16] I. García-Lodeiro, A. Palomo, A. Fernández-Jiménez, D.E. Macphee, Compatibility studies between N-A-S-H and C-A-S-H gels. Study in the ternary diagram Na_2O-CaO-Al_2O_3-SiO_2-H_2O, Cem Concr Res, 41 (2011) 923-931.

[17] C. Ruiz-Santaquiteria, J. Skibsted, A. Fernández-Jiménez, A. Palomo, Alkaline solution/binder ratio as a determining factor in the alkaline activation of aluminosilicates, Cem Concr Res, 42 (2012) 1242-1251.

[18] S.A. Bernal, J.L. Provis, B. Walkley, R. San Nicolas, J.D. Gehman, D.G. Brice, A.R. Kilcullen, P. Duxson, J.S.J. van Deventer, Gel nanostructure in alkali-activated binders based on slag and fly ash, and effects of accelerated carbonation, Cem Concr Res, 53 (2013) 127-144.

[19] R.J. Myers, S.A. Bernal, J.L. Provis, J.D. Gehman, J.S.J. van Deventer, The role of Al in cross-linking of alkali-activated slag cements, J Am Ceram Soc, 98 (2015) 996-1004.

[20] J.D. Gehman, J.L. Provis, Generalized biaxial shearing of MQMAS NMR spectra, J Magn Reson, 200 (2009) 167-172.

[21] H.M. Dyson, I.G. Richardson, A.R. Brough, A combined ^{29}Si MAS NMR and selective dissolution technique for the quantitative evaluation of hydrated blast furnace slag cement blends J Am Ceram Soc, 90 (2007) 598-602.

[22] M.R. Rowles, J.V. Hanna, K.J. Pike, M.E. Smith, B.H. O'Connor, ^{29}Si, ^{27}Al, ^{1}H and ^{23}Na MAS NMR study of the bonding character in aluminosilicate inorganic polymers, Appl Magn Reson, 32 (2007) 663-689.

[23] J. Brus, L. Kobera, M. Urbanová, D. Koloušek, J. Kotek, Insights into the structural transformations of aluminosilicate inorganic polymers: A comprehensive solid-state NMR study, J Phys Chem C, 116 (2012) 14627-14637.

[24] P. Duxson, J.L. Provis, G.C. Lukey, J.S.J. van Deventer, F. Separovic, Z.H. Gan, ^{39}K NMR of free potassium in geopolymers, Ind Eng Chem Res, 45 (2006) 9208-9210.

[25] K.J.D. MacKenzie, M.E. Smith, A. Wong, A multinuclear MAS NMR study of calcium-containing aluminosilicate inorganic polymers, J Mater Chem, 17 (2007) 5090-5096.

[26] K.J.D. MacKenzie, S. Bradley, J.V. Hanna, M.E. Smith, Magnesium analogues of aluminosilicate inorganic polymers (geopolymers) from magnesium minerals, J Mater Sci, 48 (2013) 1787-1793.

[27] A. Fernández-Jiménez, A. Palomo, Mid-infrared spectroscopic studies of alkali-activated fly ash structure, Micropor Mesopor Mater, 86 (2005) 207-214.

[28] C.A. Rees, J.L. Provis, G.C. Lukey, J.S.J. van Deventer, Attenuated total reflectance Fourier transform infrared analysis of fly ash geopolymer gel aging, Langmuir, 23 (2007) 8170-8179.

[29] W.K.W. Lee, J.S.J. van Deventer, Use of infrared spectroscopy to study geopolymerization of heterogeneous amorphous aluminosilicates, Langmuir, 19 (2003) 8726-8734.

[30] C.A. Rees, J.L. Provis, G.C. Lukey, J.S.J. van Deventer, In situ ATR-FTIR study of the early stages of fly ash geopolymer gel formation, Langmuir, 23 (2007) 9076-9082.

[31] A. Hajimohammadi, J.L. Provis, J.S.J. van Deventer, Time-resolved and spatially-resolved infrared spectroscopic observation of seeded nucleation controlling geopolymer gel formation, J Colloid Interf Sci, 357 (2011) 384-392.

[32] A. Hajimohammadi, J.L. Provis, J.S.J. van Deventer, The effect of silica availability on the mechanism of geopolymerisation, Cem Concr Res, 41 (2011) 210-216.

[33] A. Hajimohammadi, J.L. Provis, J.S.J. van Deventer, The effect of alumina release rate on the mechanism of geopolymer gel formation, Chem Mater, 22 (2010) 5199-5208.

[34] C. Meral, C.J. Benmore, P.J.M. Monteiro, The study of disorder and nanocrystallinity in C-S-H, supplementary cementitious materials and geopolymers using pair distribution function analysis, Cem Concr Res, 41 (2011) 696-710.

[35] C.E. White, Pair distribution function analysis of amorphous geopolymer precursors and binders: The importance of complementary molecular simulation, Z Kristallogr, 227 (2012) 304-312.

[36] C.E. White, J.L. Provis, B. Bloomer, N.J. Henson, K. Page, In situ X-ray pair distribution function analysis of geopolymer gel nanostructure formation kinetics, Phys Chem Chem Phys, 15 (2013) 8573-8582.

[37] C.E. White, J.L. Provis, A. Llobet, T. Proffen, J.S.J. van Deventer, Evolution of local structure in geopolymer gels: an in-situ neutron pair distribution function analysis, J Am Ceram Soc, 94 (2011) 3532-3539.

[38] C.E. White, J.L. Provis, T. Proffen, J.S.J. van Deventer, The effects of temperature on the local structure of metakaolin-based geopolymer binder: A neutron pair distribution function investigation, J Am Ceram Soc, 93 (2010) 3486-3492.

[39] C.E. White, J.L. Provis, T. Proffen, D.P. Riley, J.S.J. van Deventer, Combining density functional theory (DFT) and pair distribution function (PDF) analysis to solve the structure of metastable materials: the case of metakaolin, Phys Chem Chem Phys, 12 (2010) 3239-3245.

[40] C.E. White, L.L. Daemen, M. Hartl, K. Page, Intrinsic differences in atomic ordering of calcium (alumino)silicate hydrates in conventional and alkali-activated cements, Cem Concr Res, 67 (2015) 66-73.

[41] R.J. Myers, S.A. Bernal, R. San Nicolas, J.L. Provis, Generalized structural description of calcium-sodium aluminosilicate hydrate gels: The crosslinked substituted tobermorite model, Langmuir, 29 (2013) 5294-5306.

[42] F. Puertas, M. Palacios, H. Manzano, J.S. Dolado, A. Rico, J. Rodríguez, A model for the C-A-S-H gel formed in alkali-activated slag cements, J Eur Ceram Soc, 31 (2011) 2043-2056.

[43] R.J. Myers, S.A. Bernal, J.L. Provis, A thermodynamic model for C-(N-)A-S-H gel: CNASH_ss. Derivation and validation, Cem Concr Res, 66 (2014) 27-47.

[44] F. Deschner, B. Münch, F. Winnefeld, B. Lothenbach, Quantification of fly ash in hydrated, blended Portland cement pastes by backscattered electron imaging, J Microsc, 251 (2013) 188-204.

[45] M. Ben Haha, G. Le Saout, F. Winnefeld, B. Lothenbach, Influence of activator type on hydration kinetics, hydrate assemblage and microstructural development of alkali activated blast-furnace slags, Cem Concr Res, 41 (2011) 301-310.

[46] J. Němeček, V. Šmilauer, L. Kopecký, Nanoindentation characteristics of alkali-activated aluminosilicate materials, Cem Concr Compos, 33 (2011) 163-170.

[47] H. Xu, J.L. Provis, J.S.J. van Deventer, P.V. Krivenko, Characterization of aged slag concretes, ACI Mater J, 105 (2008) 131-139.

[48] R. San Nicolas, S.A. Bernal, R. Mejía de Gutiérrez, J.S.J. van Deventer, J.L. Provis, Distinctive microstructural features of aged sodium silicate activated slag concretes, Cem Concr Res, 65 (2014) 41-51.

[49] J.L. Provis, V. Rose, R.P. Winarski, J.S.J. van Deventer, Hard X-ray nanotomography of amorphous aluminosilicate cements, Scripta Mater, 65 (2011) 316-319.

[50] J.L. Provis, R.J. Myers, C.E. White, V. Rose, J.S.J. van Deventer, X-ray microtomography shows pore structure and tortuosity in alkali-activated binders, Cem Concr Res, 42 (2012) 855-864.

[51] S. Lee, H.-T. Jou, A. van Riessen, W.D.A. Rickard, C.-M. Chon, N.-H. Kang, Three-dimensional quantification of pore structure in coal ash-based geopolymer using conventional electron tomography, Constr Build Mater, 52 (2014) 221-226.

[52] A. Favier, G. Habert, J.B. d'Espinose de Lacaillerie, N. Roussel, Mechanical properties and compositional heterogeneities of fresh geopolymer pastes, Cem Concr Res, 48 (2013) 9-16.

[53] A. Favier, J. Hot, G. Habert, N. Roussel, J.-B. d'Espinose de Lacaillerie, Flow properties of MK-based geopolymers pastes. A comparative study with standard Portland cement pastes, Soft Matter, 10 (2014) 1134-1141.

[54] A. Poulesquen, F. Frizon, D. Lambertin, Rheological behavior of alkali-activated metakaolin during geopolymerization, J Non-Cryst Solids, 357 (2011) 3565-3571.

[55] P. Steins, A. Poulesquen, O. Diat, F. Frizon, Structural evolution during geopolymerization from an early age to consolidated material, Langmuir, 28 (2012) 8502-8510.

[56] A. Kashani, J.L. Provis, J. Xu, A.R. Kilcullen, G.G. Qiao, J.S.J. van Deventer, Effect of molecular architecture of polycarboxylate ethers on plasticizing performance in alkali activated slag paste, J Mater Sci, 49 (2014) 2761-2772.

[57] A. Kashani, J.L. Provis, G.G. Qiao, J.S.J. van Deventer, The interrelationship between surface chemistry and rheology in alkali activated slag paste, Constr Build Mater, 65 (2014) 583-591.

[58] K. Vance, A. Dakhane, G. Sant, N. Neithalath, Observations on the rheological response of alkali activated fly ash suspensions: the role of activator type and concentration, Rheol Acta, 53 (2014) 843-855.

[59] P. Gu, Z. Xu, P. Xie, J.J. Beaudoin, Application of A.C. impedance techniques in studies of porous cementitious materials. (I): Influence of solid phase and pore solution on high frequency resistance, Cem Concr Res, 23 (1993) 531-540.

[60] P. Xie, P. Gu, J.J. Beaudoin, Contact capacitance effect in measurement of a.c. impedance spectra for hydrating cement systems, J Mater Sci, 31 (1996) 144-149.

[61] X.J. Liu, C.J. Shi, F.Q. He, X. Hu, L.L. Chong, A preliminary impedance spectroscopy investigation of waterglass-activated slag cement, in: Second International Conference on Advances in Chemically-Activated Materials (CAM'2014), Changsha, China, 2014, RILEM/Springer, 290-301.

[62] W.J. McCarter, T.M. Chrisp, G. Starrs, The early hydration of alkali-activated slag: Developments in monitoring techniques, Cem Concr Compos, 21 (1999) 277-283.

[63] S. Hanjitsuwan, S. Hunpratub, P. Thongbai, S. Maensiri, V. Sata, P. Chindaprasirt, Effects of NaOH concentrations on physical and electrical properties of high calcium fly ash geopolymer paste, Cem Concr Compos, 45 (2014) 9-14.

[64] D. Ravikumar, N. Neithalath, An electrical impedance investigation into the chloride ion transport resistance of alkali silicate powder activated slag concretes, Cem Concr Compos, 44 (2013) 58-68.

[65] H.M. Jennings, J.W. Bullard, From electrons to infrastructure: Engineering concrete from the bottom up, Cem Concr Res, 41 (2011) 727-735.

[66] K. van Breugel, Modelling of cement-based systems—the alchemy of cement chemistry, Cem Concr Res, 34 (2004) 1661-1668.

[67] I.G. Richardson, Tobermorite/jennite- and tobermorite/calcium hydroxide-based models for the structure of C-S-H: applicability to hardened pastes of tricalcium silicate, β-dicalcium silicate, Portland cement, and blends of Portland cement with blast-furnace slag, metakaolin, or silica fume, Cem Concr Res, 34 (2004) 1733-1777.

[68] I.G. Richardson, Model structures for C-(A)-S-H(I), Acta Cryst B, 70 (2014) 903-923.

[69] R.J. Myers, E. L'Hôpital, J.L. Provis, B. Lothenbach, Effect of temperature and aluminium on calcium (alumino)silicate hydrate chemistry under equilibrium conditions, Cem Concr Res, 68 (2015) 83-93.

[70] D. Damidot, B. Lothenbach, D. Herfort, F.P. Glasser, Thermodynamics and cement science, Cem Concr Res, 41 (2011) 679-695.

[71] B. Lothenbach, Thermodynamic equilibrium calculations in cementitious systems, Mater Struct, 43 (2010) 1413-1433.

[72] W. Chen, H. Brouwers, The hydration of slag, part 1: reaction models for alkali-activated slag, J Mater Sci, 42 (2007) 428-443.

[73] B. Lothenbach, A. Gruskovnjak, Hydration of alkali-activated slag: Thermodynamic modelling, Adv Cem Res, 19 (2007) 81-92.

[74] S.A. Bernal, R. San Nicolas, R.J. Myers, R. Mejía de Gutiérrez, F. Puertas, J.S.J. van Deventer, J.L. Provis, MgO content of slag controls phase evolution and structural changes induced by accelerated carbonation in alkali-activated binders, Cem Concr Res, 57 (2014) 33-43.

[75] G.L. Kalousek, Studies of proportions of the quaternary system soda-lime-silica-water at 25°C, J Res Natl Bur Stand, 32 (1944) 285-302.

[76] D.E. Macphee, K. Luke, F.P. Glasser, E.E. Lachowski, Solubility and aging of calcium silicate hydrates in alkaline solutions at 25°C, J Am Ceram Soc, 72 (1989) 646-654.

[77] S.J. Way, A. Shayan, Early hydration of a portland cement in water and sodium hydroxide solutions: Composition of solutions and nature of solid phases, Cem Concr Res, 19 (1989) 759-769.

[78] Z. Zhang, H. Wang, J.L. Provis, F. Bullen, A. Reid, Y. Zhu, Quantitative kinetic and structural analysis of geopolymers. Part 1. The activation of metakaolin with sodium hydroxide, Thermochim Acta, 539 (2012) 23-33.

[79] Z. Zhang, J.L. Provis, H. Wang, F. Bullen, A. Reid, Quantitative kinetic and structural analysis of geopolymers. Part 2. Thermodynamics of sodium silicate activation of metakaolin, Thermochim Acta, 565 (2013) 163-171.

[80] V. Šmilauer, P. Hlaváček, F. Škvára, R. Šulc, L. Kopecký, J. Němeček, Micromechanical multiscale model for alkali activation of fly ash and metakaolin, J Mater Sci, 46 (2011) 6545-6555.

[81] C.E. White, J.L. Provis, G.J. Kearley, D.P. Riley, J.S.J. van Deventer, Density functional modelling of silicate and aluminosilicate dimerisation solution chemistry, Dalton Trans, 40 (2011) 1348-1355.

[82] K. Kupwade-Patil, F. Soto, A. Kunjumon, E.N. Allouche, D.S. Mainardi, Multi-scale modeling and experimental investigations of geopolymeric gels at elevated temperatures, Comput Struct, 122 (2013) 164-177.

[83] C.E. White, J.L. Provis, T. Proffen, J.S.J. van Deventer, Molecular mechanisms responsible for the structural changes occurring during geopolymerization: Multiscale simulation, AIChE J, 58 (2012) 2241-2253.

[84] S. Kumar, P. García-Triñanes, A. Teixeira-Pinto, M. Bao, Development of alkali activated cement from mechanically activated silico-manganese (SiMn) slag, Cem Concr Compos, 40 (2013) 7-13.

[85] C. Li, J. Wan, H. Sun, L. Li, Investigation on the activation of coal gangue by a new compound method, J Hazard Mater, 179 (2010) 515-520.

[86] C. Zhang, J. Xue, L. Fang, Mechanical properties and microstructures of alkali activated burned coal gangue cementitious material, J Chin Ceram Soc, 32 (2004) 1276-1280.

[87] W. Hajjaji, S. Andrejkovičová, C. Zanelli, M. Alshaaer, M. Dondi, J.A. Labrincha, F. Rocha, Composition and technological properties of geopolymers based on metakaolin and red mud, Mater Des, 52 (2013) 648-654.

[88] N. Ye, J. Yang, X. Ke, J. Zhu, Y. Li, C. Xiang, H. Wang, L. Li, B. Xiao, Synthesis and characterization of geopolymer from Bayer red mud with thermal pretreatment, J Am Ceram Soc, 97 (2014) 1652-1660.

[89] X. Ke, S.A. Bernal, N. Ye, J.L. Provis, J. Yang, One-part geopolymers based on thermally treated red mud/NaOH blends, J Am Ceram Soc, 98 (2015) 5-11.

[90] J. He, Y. Jie, J. Zhang, Y. Yu, G. Zhang, Synthesis and characterization of red mud and rice husk ash-based geopolymer composites, Cem Concr Compos, 37 (2013) 108-118.

[91] Y.-M. Zhang, S.-X. Bao, T. Liu, T.-J. Chen, J. Huang, The technology of extracting vanadium from stone coal in China: History, current status and future prospects, Hydrometall, 109 (2011) 116-124.

[92] X. Jiao, Y. Zhang, T. Chen, Thermal stability of a silica-rich vanadium tailing based geopolymer, Constr Build Mater, 38 (2013) 43-47.

[93] L. Zhang, S. Ahmari, J. Zhang, Synthesis and characterization of fly ash modified mine tailings-based geopolymers, Constr Build Mater, 25 (2011) 3773-3781.

[94] M.M. Tashima, J.L. Akasaki, V.N. Castaldelli, L. Soriano, J. Monzó, J. Payá, M.V. Borrachero, New geopolymeric binder based on fluid catalytic cracking catalyst residue (FCC), Mater Lett, 80 (2012) 50-52.

[95] E.D. Rodríguez, S.A. Bernal, J.L. Provis, J.D. Gehman, J.M. Monzó, J. Payá, M.V. Borrachero, Geopolymers based on spent catalyst residue from a fluid catalytic cracking (FCC) process, Fuel, 109 (2013) 493-502.

[96] J.J. Trochez, R. Mejía de Gutiérrez, J. Rivera, S.A. Bernal, Synthesis of geopolymer from FCC: Effect of SiO_2/Al_2O_3 and Na_2O/SiO_2 molar ratios, Mater Constr, 65 (2015), article e046, DOI 10.3989/mc.2015.00814.

[97] I.B. Topçu, M.U. Toprak, Properties of geopolymer from circulating fluidized bed combustion coal bottom ash, Mater Sci Eng A, 528 (2011) 1472-1477.

[98] A. Sathonsaowaphak, P. Chindaprasirt, K. Pimraksa, Workability and strength of lignite bottom ash geopolymer mortar, J Hazard Mater, 168 (2009) 44-50.

[99] S. Donatello, O. Maltseva, A. Fernandez-Jimenez, A. Palomo, The early age hydration reactions of a hybrid cement containing a very high content of coal bottom ash, J Am Ceram Soc, 97 (2014) 929-937.

[100] S. Detphan, P. Chindaprasirt, Preparation of fly ash and rice husk ash geopolymer, Int J Miner Metall Mater, 16 (2009) 720-726.

[101] S.A. Bernal, E.D. Rodríguez, R. Mejía de Gutierrez, J.L. Provis, S. Delvasto, Activation of metakaolin/slag blends using alkaline solutions based on chemically modified silica fume and rice husk ash, Waste Biomass Valoriz, 3 (2012) 99-108.

[102] Y. Zarina, A.M. Mustafa Al Bakri, H. Kamarudin, I. Khairul Nazar, A.R. Rafiza, Review on the various ash from palm oil waste as geopolymer material, Rev Adv Mater Sci, 34 (2013) 37-43.

[103] M.A. Salih, A.A. Abang Ali, N. Farzadnia, Characterization of mechanical and microstructural properties of palm oil fuel ash geopolymer cement paste, Constr Build Mater, 65 (2014) 592-603.

[104] N. Ranjbar, M. Mehrali, U.J. Alengaram, H.S.C. Metselaar, M.Z. Jumaat, Compressive strength and microstructural analysis of fly ash/palm oil fuel ash based geopolymer mortar under elevated temperatures, Constr Build Mater, 65 (2014) 114-121.

[105] M.M. Tashima, L. Soriano, M.V. Borrachero, J. Monzó, C.R. Cheeseman, J. Payá, Alkali activation of vitreous calcium aluminosilicate derived from glass fiber waste, J Sust Cem-Based Mater, 1 (2012) 83-93.

[106] A. Balaguer Pascual, M.T. Tognonvi, A. Tagnit-Hamou, Waste glass powder-based alkali-activated mortar, Int J Res Eng Technol, 3 (2014) 32-36.

[107] D. Bajare, G. Bumanis, A. Korjakins, New porous material made from industrial and municipal waste for building application, Mater Sci (Medžiagotyra), 20 (2014) 333-338.

[108] F. Puertas, M. Torres-Carrasco, Use of glass waste as an activator in the preparation of alkali-activated slag. Mechanical strength and paste characterisation, Cem Concr Res, 57 (2014) 95-104.

[109] L. Reig, M.M. Tashima, L. Soriano, M.V. Borrachero, J. Monzó, J. Payá, Alkaline activation of ceramic waste materials, Waste Biomass Valor, 4 (2013) 729-736.

[110] P. Banfill, M. Frias, Rheology and conduction calorimetry of cement modified with calcined paper sludge, Cem Concr Res, 37 (2007) 184-190.

[111] R.A. Antunes Boca Santa, A.M. Bernardin, H.G. Riella, N.C. Kuhnen, Geopolymer synthetized from bottom coal ash and calcined paper sludge, J Cleaner Prod, 57 (2013) 302-307.

[112] K.-H. Yang, C.-W. Lo, J.-S. Huang, Production and properties of foamed reservoir sludge inorganic polymers, Cem Concr Compos, 38 (2013) 50-56.

[113] X.L. Guo, H.S. Shi, W. Dick, Use of heat-treated water treatment residuals in fly ash-based geopolymers, J Am Ceram Soc, 93 (2010) 272-278.

[114] D. Feng, J.L. Provis, J.S.J. van Deventer, Thermal activation of albite for the synthesis of one-part mix geopolymers, J Am Ceram Soc, 95 (2012) 565-572.

[115] M.D. Jackson, E.N. Landis, P.F. Brune, M. Vitti, H. Chen, Q. Li, M. Kunz, H.-R. Wenk, P.J.M. Monteiro, A.R. Ingraffea, Mechanical resilience and cementitious processes in Imperial Roman architectural mortar, Proc Nat Acad Sci USA, 111 (2014) 18484–18489.

[116] E. Najafi Kani, A. Allahverdi, J.L. Provis, Efflorescence control in geopolymer binders based on natural pozzolan, Cem Concr Compos, 34 (2012) 25-33.

[117] E. Najafi Kani, A. Allahverdi, Effect of chemical composition on basic engineering properties of inorganic polymeric binder based on natural pozzolan, Ceram-Silik, 53 (2009) 195-204.

[118] E. Kamseu, Z.N.M. Ngouloure, B.N. Ali, S. Zekeng, U.C. Melo, D.S. Rossignol, C. Leonelli, Cumulative pore volume, pore size distribution and phases percolation in porous inorganic polymer composites: Relation microstructure and effective thermal conductivity, Energy Build, 88 (2015) 45-56.

[119] P.N. Lemougna, K.J.D. MacKenzie, G.N.L. Jameson, H. Rahier, U.F. Chinje Melo, The role of iron in the formation of inorganic polymers (geopolymers) from volcanic ash: a ^{57}Fe Mössbauer spectroscopy study, J Mater Sci, 48 (2013) 5280-5286.

[120] H.K. Tchakoute, A. Elimbi, E. Yanne, C.N. Djangang, Utilization of volcanic ashes for the production of geopolymers cured at ambient temperature, Cem Concr Compos, 38 (2013) 75-81.

[121] A. Fernández-Jiménez, A. Palomo, Characterisation of fly ashes. Potential reactivity as alkaline cements., Fuel, 82 (2003) 2259-2265.

[122] D.P. Bentz, A.S. Hansen, J.M. Guynn, Optimization of cement and fly ash particle sizes to produce sustainable concretes, Cem Concr Compos, 33 (2011) 824-831.

[123] S. Kumar, R. Kumar, Mechanical activation of fly ash: Effect on reaction, structure and properties of resulting geopolymer, Ceram Int, 37 (2011) 533-541.

[124] I. Garcia-Lodeiro, A. Fernandez-Jimenez, A. Palomo, Hydration kinetics in hybrid binders: Early reaction stages, Cem Concr Compos, 39 (2013) 82-92.

[125] S.A. Bernal, D. Herfort, J. Skibsted, Novel hybrid binders based on alkali sulfate-activated portland clinker and metakaolin, in: 13th International Congress on the Chemistry of Cement, Madrid, Spain, 2011, CD-ROM proceedings.

[126] M.J. Sánchez-Herrero, A. Fernández-Jiménez, A. Palomo, Alkaline hydration of tricalcium aluminate, J Am Ceram Soc, 95 (2012) 3317-3324.

[127] M.J. Sánchez-Herrero, A. Fernández-Jiménez, A. Palomo, $C_4A_3\check{S}$ hydration in different alkaline media, Cem Concr Res, 46 (2013) 41-49.

[128] G. Li, P. Le Bescop, M. Moranville, The U phase formation in cement-based systems containing high amounts of Na_2SO_4, Cem Concr Res, 26 (1996) 27-33.

[129] M.J. Sanchez Herrero, Ph.D Thesis, Universidad Nacional de Educación a Distancia, Madrid, Spain, 2015.

[130] C. Shi, Characteristics and cementitious properties of ladle slag fines from steel production, Cem Concr Res, 32 (2002) 459-462.

[131] L. Kriskova, Y. Pontikes, F. Zhang, Ö. Cizer, P.T. Jones, K. Van Balen, B. Blanpain, Influence of mechanical and chemical activation on the hydraulic properties of gamma dicalcium silicate, Cem Concr Res, 55 (2014) 59-68.

[132] A. Fernández-Jiménez, F. Zibouche, N. Boudissa, I. García-Lodeiro, M.T. Abadlia, A. Palomo, "Metakaolin-slag-clinker blends." The role of Na^+ or K^+ as alkaline activators of these ternary blends, J Am Ceram Soc, 96 (2013) 1991-1998.

[133] K. Arbi, A. Palomo, A. Fernández-Jiménez, Alkali-activated blends of calcium aluminate cement and slag/diatomite, Ceram Int, 39 (2013) 9237-9245.

[134] R.M. Barrer, Hydrothermal Chemistry of Zeolites, Academic Press, London, 1982.

[135] A. Dyer, An Introduction to Zeolite Molecular Sieves, John Wiley & Sons, Chichester, 1988.

[136] P.V. Krivenko, Alkaline cements, in: Proceedings of the First International Conference on Alkaline Cements and Concretes, Kiev, Ukraine, 1994, 11-129.

[137] E. Douglas, A. Bilodeau, V.M. Malhotra, Properties and durability of alkali-activated slag concrete, ACI Mater J, 89 (1992) 509-516.

[138] S.A. Bernal, R. Mejía de Gutiérrez, J.L. Provis, Engineering and durability properties of concretes based on alkali-activated granulated blast furnace slag/metakaolin blends, Constr Build Mater, 33 (2012) 99-108.

[139] I. Ismail, S.A. Bernal, J.L. Provis, R. San Nicolas, D.G. Brice, A.R. Kilcullen, S. Hamdan, J.S.J. van Deventer, Influence of fly ash on the water and chloride permeability of alkali-activated slag mortars and concretes, Constr Build Mater, 48 (2013) 1187-1201.

[140] C. Shi, J.A. Stegemann, R.J. Caldwell, Effect of supplementary cementing materials on the Rapid Chloride Permeability Test (AASHTO T 277 and ASTM C1202) results, ACI Mater J, 95 (1998) 389-394.

[141] C. Shi, Strength, pore structure and permeability of alkali-activated slag mortars, Cem Concr Res, 26 (1996) 1789-1799.

[142] Nordtest, Concrete, mortar and cement-based repair materials: Chloride migration coefficient from non-steady state migration experiments (NT BUILD 492), Espoo, Finland, 1999.

[143] ASTM International, Standard Test Method for Determining the Penetration of Chloride Ion into Concrete by Ponding (ASTM C1543-10a), West Conshohocken, PA, 2010.

[144] F. He, C. Shi, Q. Yuan, X. An, B. Tong, Calculation of chloride concentration at color change boundary of $AgNO_3$ colorimetric measurement, Cem Concr Res, 41 (2011) 1095-1103.

[145] Q. Yuan, C. Shi, F. He, G. De Schutter, K. Audenaert, K. Zheng, Effect of hydroxyl ions on chloride penetration depth measurement using the colorimetric method, Cem Concr Res, 38 (2008) 1177-1180.

[146] F. He, C. Shi, C. Chen, X. An, B. Tong, Error analysis for measurement of non-steady state chloride migration coefficient in concrete using $AgNO_3$ colorimetric method, J Chin Ceram Soc, 40 (2012) 20-26.

[147] M.S. Badar, K. Kupwade-Patil, S.A. Bernal, J.L. Provis, E.N. Allouche, Corrosion of steel bars induced by accelerated carbonation in low and high calcium fly ash geopolymer concretes, Constr Build Mater, 61 (2014) 79-89.

[148] M. Criado, C. Monticelli, S. Fajardo, D. Gelli, V. Grassi, J.M. Bastidas, Organic corrosion inhibitor mixtures for reinforcing steel embedded in carbonated alkali-activated fly ash mortar, Constr Build Mater, 35 (2012) 30-37.

[149] C. Monticelli, M. Criado, S. Fajardo, J.M. Bastidas, M. Abbottoni, A. Balbo, Corrosion behaviour of a low Ni austenitic stainless steel in carbonated chloride-polluted alkali-activated fly ash mortar, Cem Concr Res, 55 (2014) 49-58.

[150] S.A. Bernal, The resistance of alkali-activated cement-based binders to carbonation, in: F. Pacheco-Torgal, J.A. Labrincha, C. Leonelli, A. Palomo, P. Chindaprasirt (Eds.) Handbook of Alkali-Activated Cements, Mortars and Concretes, Woodhead, Cambridge, UK, 2015, pp. 319-332.

[151] A. Morandeau, M. Thiéry, P. Dangla, Investigation of the carbonation mechanism of CH and C-S-H in terms of kinetics, microstructure changes and moisture properties, Cem Concr Res, 56 (2014) 153-170.

[152] F. Puertas, M. Palacios, T. Vázquez, Carbonation process of alkali-activated slag mortars, J Mater Sci, 41 (2006) 3071-3082.

[153] S.A. Bernal, R. Mejía de Gutierrez, V. Rose, J.L. Provis, Effect of silicate modulus and metakaolin incorporation on the carbonation of alkali silicate-activated slags, Cem Concr Res, 40 (2010) 898-907.

[154] M. Criado, A. Palomo, A. Fernández-Jiménez, Alkali activation of fly ashes. Part 1: Effect of curing conditions on the carbonation of the reaction products, Fuel, 84 (2005) 2048-2054.

[155] European Committee for Standardization (CEN), Products and systems for the protection and repair of concrete structures – test methods – Determination of resistance to carbonation (EN 13295:2004), Brussels, Belgium, 2004.

[156] S.A. Bernal, J.L. Provis, R. Mejía de Gutiérrez, J.S.J. van Deventer, Accelerated carbonation testing of alkali-activated slag/metakaolin blended concretes: effect of exposure conditions, Mater Struct, 48 (2015) 653-669.

[157] S.A. Bernal, J.L. Provis, D.G. Brice, A. Kilcullen, P. Duxson, J.S.J. van Deventer, Accelerated carbonation testing of alkali-activated binders significantly underestimates service life: The role of pore solution chemistry, Cem Concr Res, 42 (2012) 1317-1326.

[158] P.J.M. Monteiro, Scaling and saturation laws for the expansion of concrete exposed to sulfate attack, Proc Natl Acad Sci USA, 103 (2006) 11467-11472.

[159] A.M. Rashad, Y. Bai, P.A.M. Basheer, N.B. Milestone, N.C. Collier, Hydration and properties of sodium sulfate activated slag, Cem Concr Compos, 37 (2013) 20-29.

[160] T. Bakharev, Durability of geopolymer materials in sodium and magnesium sulfate solutions, Cem Concr Res, 35 (2005) 1233-1246.

[161] S. Thokchom, P. Ghosh, S. Ghosh, Performance of fly ash based geopolymer mortars in sulphate solution, J Eng Sci Technol Rev, 3 (2010) 36-40.

[162] I. Ismail, S.A. Bernal, J.L. Provis, S. Hamdan, J.S.J. van Deventer, Microstructural changes in alkali activated fly ash/slag geopolymers with sulfate exposure, Mater Struct, 46 (2013) 361-373.

[163] C. Desbats-Le Chequer, F. Frizon, Impact of sulfate and nitrate incorporation on potassium- and sodium-based geopolymers: geopolymerization and materials properties, J Mater Sci, 46 (2011) 5657-5664.

[164] N. Mobasher, S.A. Bernal, O.H. Hussein, D.C. Apperley, H. Kinoshita, J.L. Provis, Characterisation of $Ba(OH)_2$-Na_2SO_4-blast furnace slag cement-like composites for the immobilisation of sulphate bearing nuclear wastes, Cem Concr Res, 66 (2014) 64-74.

[165] C. Shi, Corrosion resistance of alkali-activated slag cement, Adv Cem Res, 15 (2003) 77-81.

[166] R.R. Lloyd, J.L. Provis, J.S.J. van Deventer, Acid resistance of inorganic polymer binders. 1. Corrosion rate, Mater Struct, 45 (2012) 1-14.

[167] S.A. Bernal, E.D. Rodríguez, R. Mejía de Gutiérrez, J.L. Provis, Performance of alkali-activated slag mortars exposed to acids, J Sust Cem-Based Mater, 1 (2012) 138-151.

[168] X. Pu, C. Yang, F. Liu, Studies on resistance of alkali activated slag concrete to acid attack, in: Proceedings of the Second International Conference on Alkaline Cements and Concretes, Kiev, Ukraine, 1999, 717-721.

[169] C. Shi, J.A. Stegemann, Acid corrosion resistance of different cementing materials, Cem Concr Res, 30 (2000) 803-808.

[170] A. Fernández-Jiménez, I. García-Lodeiro, A. Palomo, Durability of alkali-activated fly ash cementitious materials, J Mater Sci, 42 (2007) 3055-3065.

[171] C. Shi, S. Z., X. Hu, R. Zhao, L. Chong, A review on alkali-aggregate reactions in alkali-activated mortars/ concretes made with alkali-reactive aggregates, Mater Struct, 48 (2015) 621-628.

[172] M. Thomas, The effect of supplementary cementing materials on alkali-silica reaction: A review, Cem Concr Res, 41 (2011) 1224-1231.

[173] P.M. Gifford, J.E. Gillott, Alkali-silica reaction (ASR) and alkali-carbonate reaction (ACR) in activated blast furnace slag cement (ABFSC) concrete, Cem Concr Res, 26 (1996) 21-26.

[174] C. Yang, X. Pu, F. Wu, Research on alkali aggregate reaction expansion of alkali-slag mortar, J Chin Ceram Soc, 27 (1999) 651-657.

[175] P. Krivenko, R. Drochytka, A. Gelevera, E. Kavalerova, Mechanism of preventing the alkali-aggregate reaction in the alkali activated cement concretes, Cem Concr Compos, 45 (2014) 157-165.

[176] Z. Shi, S. C., R. Zhao, S. Wan, Comparison of alkali-silica reactions in alkali-activated slag and Portland cement mortars, Mater Struct, 48 (2015) 743-751.

[177] P.V. Krivenko, A. Gelevera, V. Fedorenko, The effect of alkali on destructive and constructive processes during alkali aggregate reaction, in: First International Conference on Advances in Chemically-Activated Materials, Jinan, China, 2010, RILEM/Springer, 140-147.

[178] D. Lu, Y. Liu, Z. Xu, ASR behavior of various glass aggregates in geopolymer mortars, in: Second International Conference on Advances in Chemically-Activated Materials (CAM'2014), Changsha, China, 2014, RILEM/Springer, 376-384.

[179] T. Ichikawa, Alkali–silica reaction, pessimum effects and pozzolanic effect, Cem Concr Res, 39 (2009) 716-726.

[180] ASTM International, Standard Test Method for Potential Alkali Reactivity of Aggregates (Mortar-Bar Method) (ASTM C1260 - 07), West Conshohocken, PA, 2007.

[181] R.R. Lloyd, J.L. Provis, J.S.J. van Deventer, Pore solution composition and alkali diffusion in inorganic polymer cement, Cem Concr Res, 40 (2010) 1386-1392.

[182] Z. Xie, W. Xiang, Y. Xi, ASR potentials of glass aggregates in water-glass activated fly ash and Portland cement mortars, J Mater Civil Eng, 15 (2003) 67-74.

[183] C. Shi, Study on alkali activated phosphorus slag cement, J Nanjing Inst Chem Technol, 10 (1988) 110-116.

[184] K.J.D. MacKenzie, The secret life of inorganic polymers, CIMTEC 2014, Montecatini Terme, Italy, 2014.

[185] A. Buchwald, M. Vanooteghem, E. Gruyaert, H. Hilbig, N. Belie, Purdocement: application of alkali-activated slag cement in Belgium in the 1950s, Mater Struct, 48 (2015) 501-511.

[186] A. Palomo, A. Fernández-Jiménez, C. López-Hombrados, J.L. Lleyda, Railway sleepers made of alkali activated fly ash concrete, Rev Ing Constr, 22 (2007) 75-80.

[187] J.L. Bell, P.E. Driemeyer, W.M. Kriven, Formation of ceramics from metakaolin-based geopolymers. Part II: K-based geopolymer, J Am Ceram Soc, 92 (2009) 607-615.

[188] J.L. Bell, P.E. Driemeyer, W.M. Kriven, Formation of ceramics from metakaolin-based geopolymers: Part I - Cs-based geopolymer, J Am Ceram Soc, 92 (2009) 1-8.

[189] C. Kuenzel, L.M. Grover, L. Vandeperre, A.R. Boccaccini, C.R. Cheeseman, Production of nepheline/quartz ceramics from geopolymer mortars, J Eur Ceram Soc, 33 (2013) 251-258.

[190] Z. Zhang, J.L. Provis, A. Reid, H. Wang, Geopolymer foam concrete: an emerging material for sustainable construction, Constr Build Mater, 56 (2014) 113-127.

[191] E. Kamseu, B. Nait-Ali, M.C. Bignozzi, C. Leonelli, S. Rossignol, D.S. Smith, Bulk composition and microstructure dependence of effective thermal conductivity of porous inorganic polymer cements, J Eur Ceram Soc, 32 (2012) 1592-1603.

[192] E. Prud'homme, P. Michaud, E. Joussein, C. Peyratout, A. Smith, S. Arrii-Clacens, J.M. Clacens, S. Rossignol, Silica fume as porogent agent in geo-materials at low temperature, J Eur Ceram Soc, 30 (2010) 1641-1648.

[193] M.T. Muhammad Faheem, A.M. Mustafa Al Bakri, C.M. Ruzaidi, M. Bnhussain, H. Kamarudin, S. Mohammad Tamizi, A.M. Izzat, A. Alida, Development of pilot plant for novel geopolymer brick making machine, Adv Environ Biol, 7 (2013) 3611-3616.

[194] S. Ahmari, L. Zhang, Production of eco-friendly bricks from copper mine tailings through geopolymerization, Constr Build Mater, 29 (2012) 323-331.

[195] A. Kumar, S. Kumar, Development of paving blocks from synergistic use of red mud and fly ash using geopolymerization, Constr Build Mater, 38 (2013) 865-871.

[196] H.G. van Oss, A.C. Padovani, Cement manufacture and the environment. Part II: Environmental challenges and opportunities, J Industr Ecol, 7 (2003) 93-126.

[197] M. Weil, K. Dombrowski-Daube, A. Buchwald, Geopolymer binders – Part 3: Ecological and economic analyses of geopolymer concrete mixes for external structural elements, ZKG Int, (2011) 76-87.

[198] B.C. McLellan, R.P. Williams, J. Lay, A. van Riessen, G.D. Corder, Costs and carbon emissions for Geopolymer pastes in comparison to Ordinary Portland Cement, J Cleaner Prod, 19 (2011) 1080-1090.

[199] G. Habert, J.B. d'Espinose de Lacaillerie, N. Roussel, An environmental evaluation of geopolymer based concrete production: reviewing current research trends, J Cleaner Prod, 19 (2011) 1229-1238.

[200] P. Duxson, J.L. Provis, G.C. Lukey, J.S.J. van Deventer, The role of inorganic polymer technology in the development of 'Green concrete', Cem Concr Res, 37 (2007) 1590-1597.

[201] Y. Yao, Y. Li, X. Liu, H. Sun, S. Jiang, C. Feng, Performance and energy calculation on a green cementitious material composed of coal refuse, Clean Techn Environ Policy, 16 (2014) 281-290.